Modern Solid State NMR Techniques for the Study of Molecular Solids

Hellmut Eckert

Institut für Physikalische Chemie
WWU Münster, Germany
&
Instituto de Física, Sao Carlos
Universidade de Sao Paulo, Brasil

Current Research Agenda

H. Eckert
eckert@ifsc.usp.br

NMR Methods Development	Glass Science	Li Ion Battery Components	Optical Materials	Catalysts Biomaterials
SSNMR, ESR Dipolar Techniques	Structure Dynamics, Sol-Gel	Electrode Electrolytes, Ceramics	Luminescent Ceramics, Hybrids	FLP, Zeolite Nanocomposites Bioceramics

Support

Industry: Corning, Schott, Ivoclar, Nippon Glass
DFG, DFG-SFB, IRTG, BMBF
CNPq Universal, FAPESP, CEPID, CNPq

Outline

Solid State NMR – General Aspects

Anisotropic Interactions:

- magnetic shielding
- dipole-dipole coupling
- nuclear electric quadrupole coupling

Manipulation of Interactions

- high-resolution NMR in crystalline Systems
- dipolar spectroscopy
- cross-polarization

NMR Studies of Insensitive Nuclei

NMR Studies of Supramolecular Systems

NMR Studies of Frustrated Lewis Pairs

Literature

Highlight articles

D. Laws, H. M. Bitter, A. Jerschow, Angew. Chem. Int. Ed. 41 (2002), 3096.
M. J. Duer, Ann. Rep. NMR Spectrosc. 43 (2000), 1.

Fundamental Principles (Theory)

A. Abragam, *The Principles of Nuclear Magnetism*, Clarendon Press Oxford (1961).
C. P. Slichter, *Principles of Magnetic Resonance*, Springer Verlag Heidelberg 1978.
B.C. Gerstein, C.R. Dybowski, *Transient Techniques in NMR of Solids*, Academic Press Inc (1985).
M. Mehring, *Principles of High Resolution NMR in Solids*, Springer Verlag Heidelberg (1983)
R.R. Ernst, G. Bodenhausen, A. Wokaun, *Principles of Nuclear Magnetic Resonance in One and Two Dimensions*, Clarendon Press, Oxford (1987)

NMR Applications to Materials Sciences

J. Klinowski, Ed. *New Techniques in Solid State NMR*, Topics in Current Chemistry, 246, Springer-Verlag Heidelberg 2005.
K. Schmidt-Rohr, H.W. Spiess, Multidimensional *Solid-State NMR and Polymers*, Academic Press, London (1996).
M. J. Duer, *Introduction into Solid State NMR Spectroscopy*, Blackwell Publ. 2004

NMR = Nuclear Magnetic Resonance

N: Property of the Atomic Nuclei in Matter

M: Magnetic Property, arising from Spin Angular Momentum

R: Interaction with electromagnetic waves spectroscopy

Relationship Spin-magnetic moment

Classical model: charge q on a circle with radius r

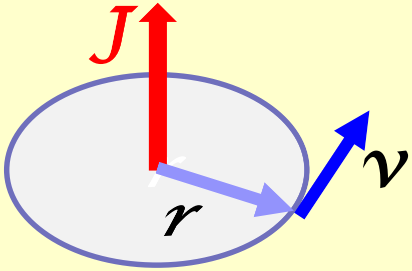

Magnetic moment: μ = current $\times$ area

Charge q on a circle: velocity: $v = 2\pi r/t$ -> $t = 2\pi r/v$

current = $q/t = qv/2\pi r$
area = πr^2

} $\mu = q\,v\,r/2$

Angular momentum: $J = p \times r = m\,v\,r$
Magnetic moment: $\mu = J\,q/2m$ (classical)
$\mu = J\,\gamma$ (quantum mechanical)

γ: *gyromagnetic ratio* (units $T^{-1}s^{-1}$)

Magnetic moments interact with magnetic fields

Zeeman interaction: E = - μ B

B is called „magnetic flux density“ and characterizes the strength of the magnetic field: units 1Tesla = Vs/m^2

Orientational quantization of spin: $|S_z| = m\ h/2\pi$

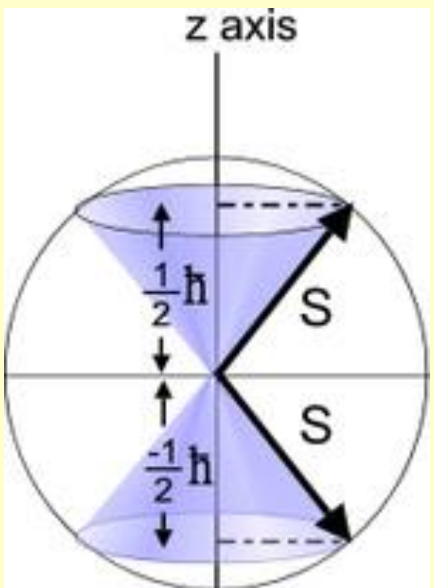

F = -dE/dz = - μ (dB/dz) cos(μ,B)

In an inhomogeneous magnetic field (magnetic field gradient) different spin orientations experience forces of different strengths

Case spin-1/2: Two nuclear spin orientations

$E(m) = - m\gamma\hbar B_0$ (Zeeman-interaction)

The two orientations have different energies, difference depends on the values of B_0 and γ

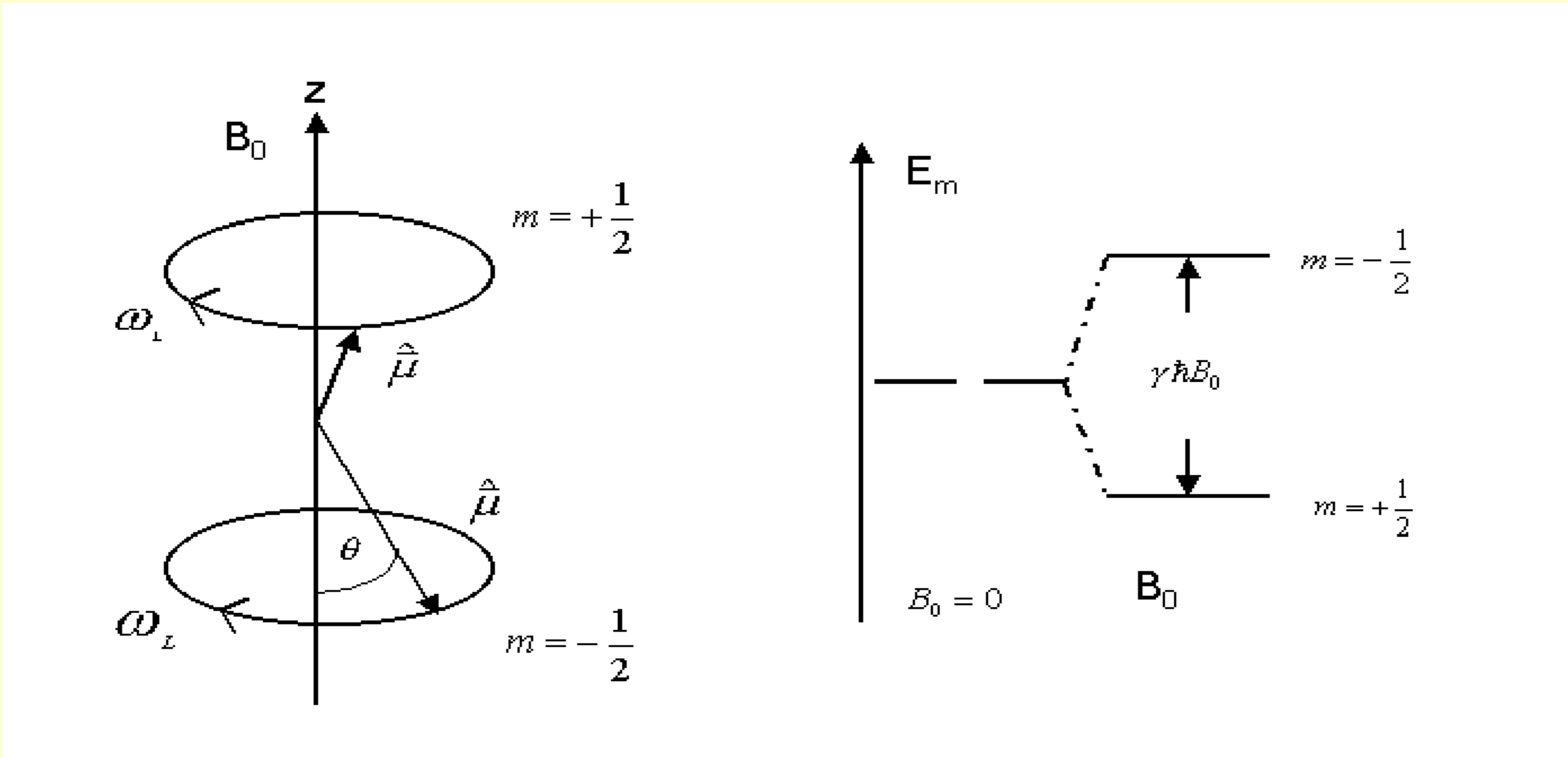

Stern - Gerlach experiment

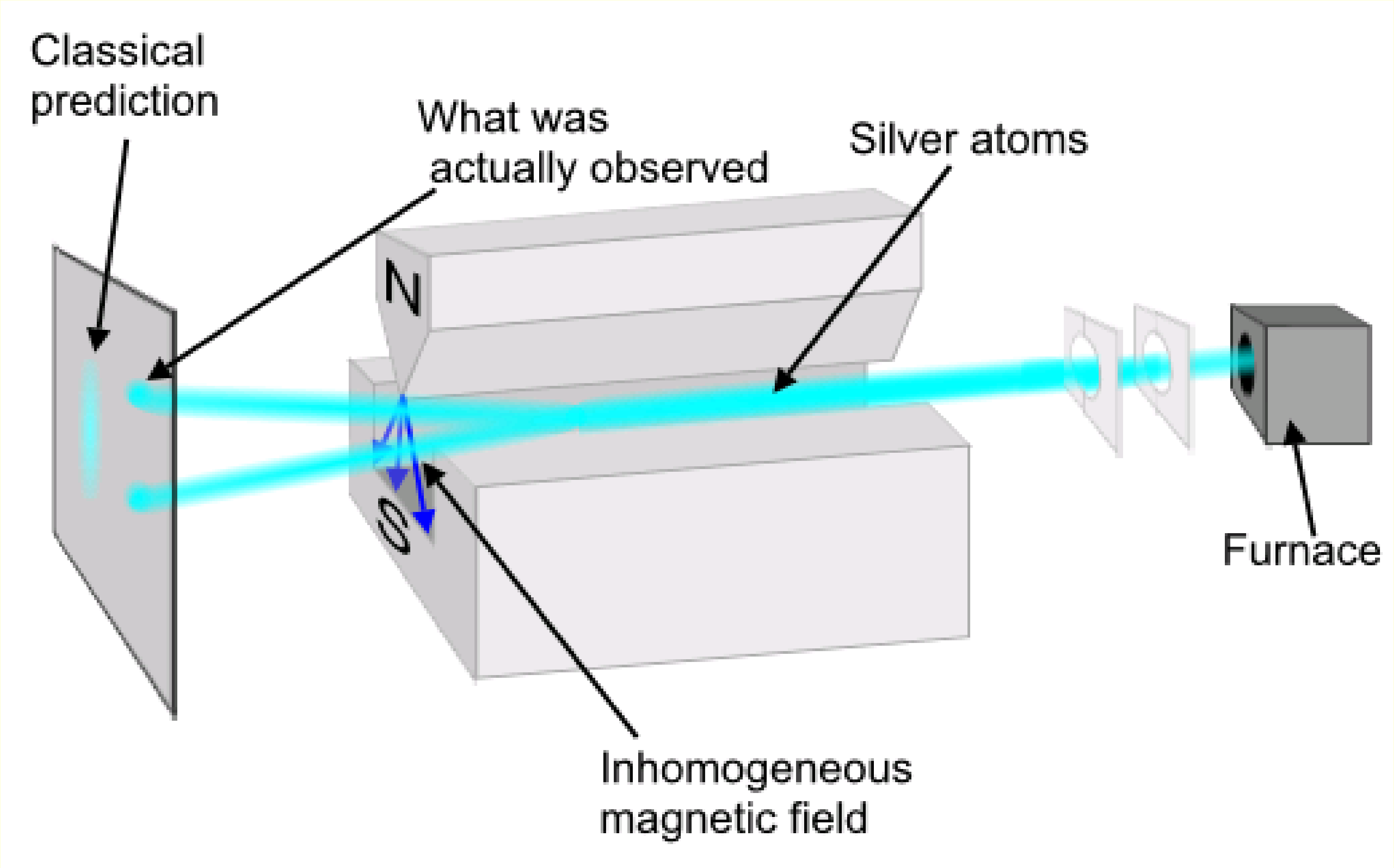

The Stern – Gerlach experiment, 1922

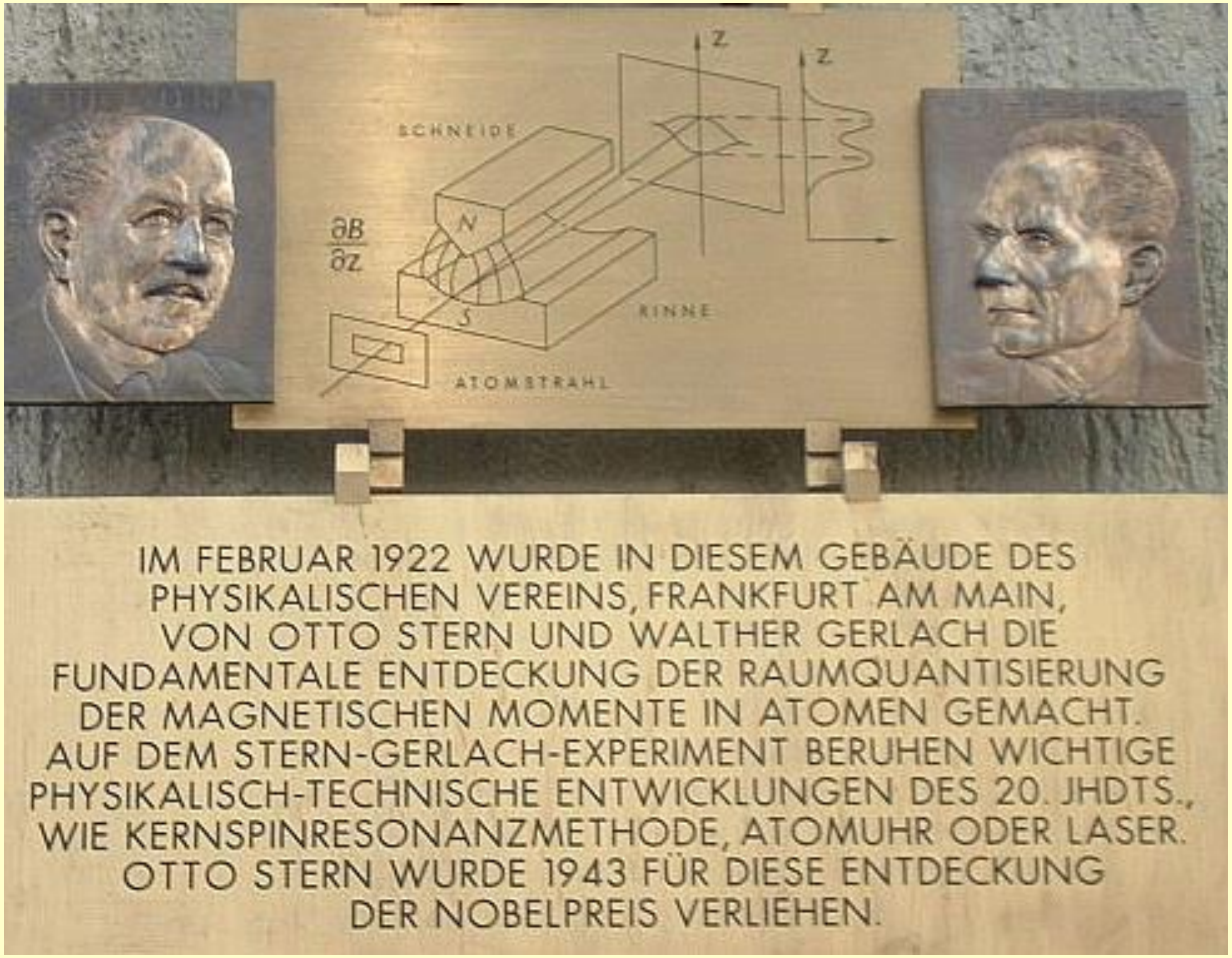

Experiment of Rabi

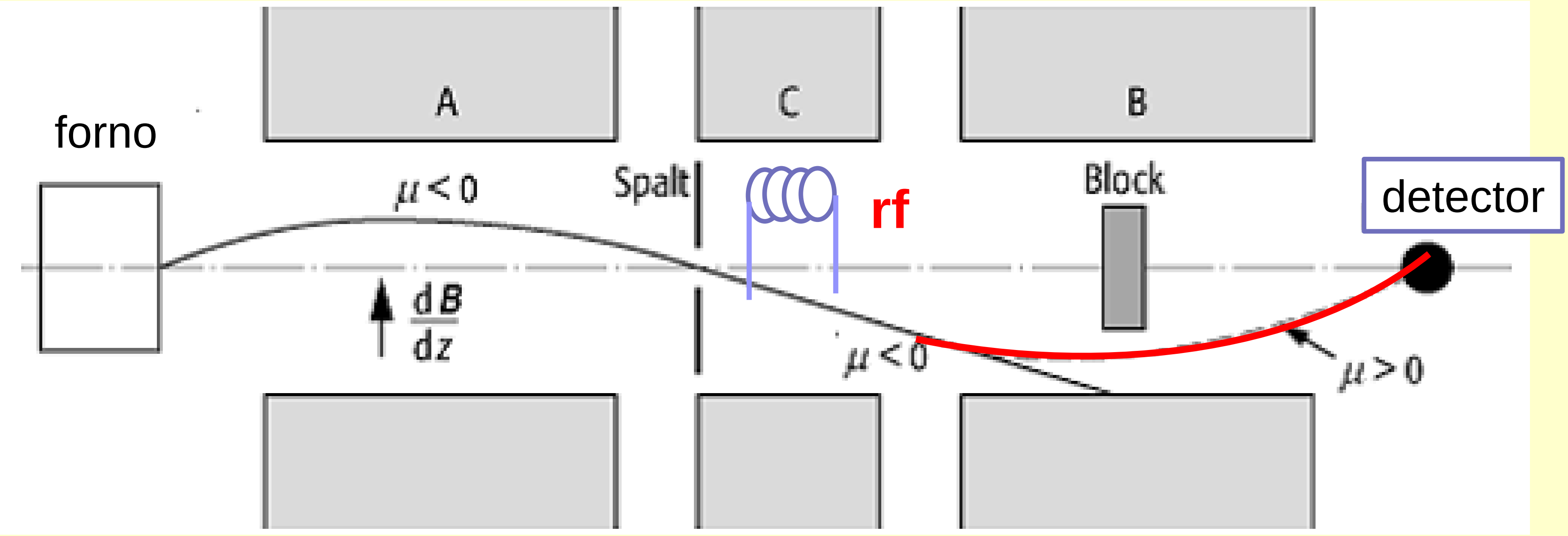

Resonance: $\omega = \gamma B_o$

History *

1922 **Stern-Gerlach** Experiment
1938 **Rabi-** Experiment
1945/46 **Purcell/Pound, Bloch**: first NMR in cond. matter
1948 **Bloembergen, Purcell, Pound**: relaxation
1948 **Pake, van-Vleck**: dipolar analysis
1949 **KNIGHT** shift in metals
1950 **Dickinson, Proctor, Yu**: chemical shift
1950-s: commercial spectrometers (VARIAN)
1952 **Gutowsky, Slichter** spin-spin coupling
1950s **Hahn, Slichter**, pulsed NMR, spin echo

* **Nobel laureates**

Important milestones

1958	**Andrew:** magic-angle sample spinning
1966	**Ernst, Anderson**: pulsed Fourier Transf. NMR
early 1970-s	**Lauterbur, Mansfield**: NMR Imaging
early 1970s	**Jeener, Ernst, Bax**: 2-D NMR
1970-s	**Wüthrich**: Protein structure solutions
1975	**Schaefer:** cross-polarization
1980-s	**Spiess:** Polymer dynamics via NMR
1985	**Weitekamp:** Para Hydrogen polarizaiton
1989	**Pines:** Xe- and He Hyperpolarizaiton
1990	**Tycko:** Laser polarization
1990-s	**Griffin, Levitt, S. Vega**: multipulse NMR 1995
	Frydman: High-res. NMR of Q-nuclei
2000:	**Nielsen:** SIMPSON software
2000-s:	High-field magnet technology-> 23.6 T
2000-s:	**Kutzelnigg, Gauss, Schwarz:** DFT-calculations
2000-s	**Griffin, Emsley, Bodenhausen**: DNP/MAS

Nuclear Magnetism

Nuclear magnetic moment: $\mu = \gamma \hat{J} = \gamma \hbar \hat{I}$

I, the angular momentum, is subject to quantization laws, concerning both magnitude and orientation

$$\hat{\vec{\mathbf{I}}}^2 |I, m\rangle = \mathrm{I}(\mathrm{I}+1)|I, m\rangle$$

$$\hat{\mathrm{I}}_z |I, m\rangle = \mathrm{m}|I, m\rangle$$

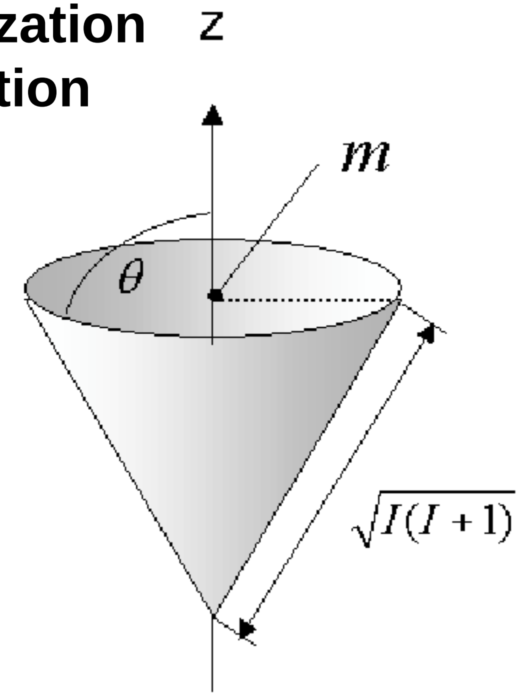

$\cos\theta = m / \sqrt{I(I+1)}$

I: spin quantum number

m: orientational quantum number
with m=-I,-I+1,…I-1,I
2I +1 orientational states

Nuclear spin quantum numbers

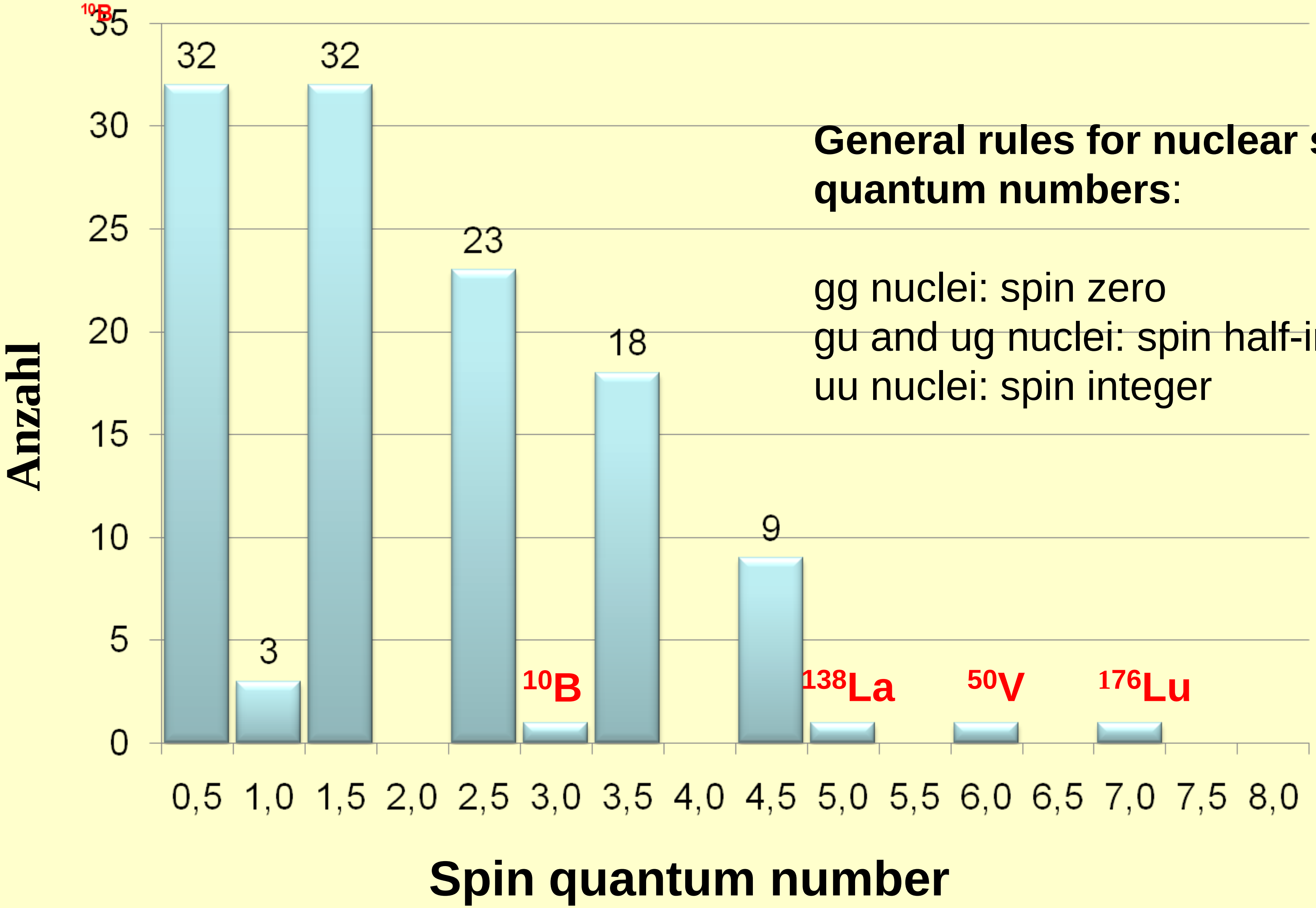

General rules for nuclear spin quantum numbers:

gg nuclei: spin zero
gu and ug nuclei: spin half-integer
uu nuclei: spin integer

Case spin-1/2: Two nuclear spin orientations

$E(m) = -m\gamma\hbar B_0$ (Zeeman-interaction)

→ The two orientations have different energies, difference depends on the value of γ

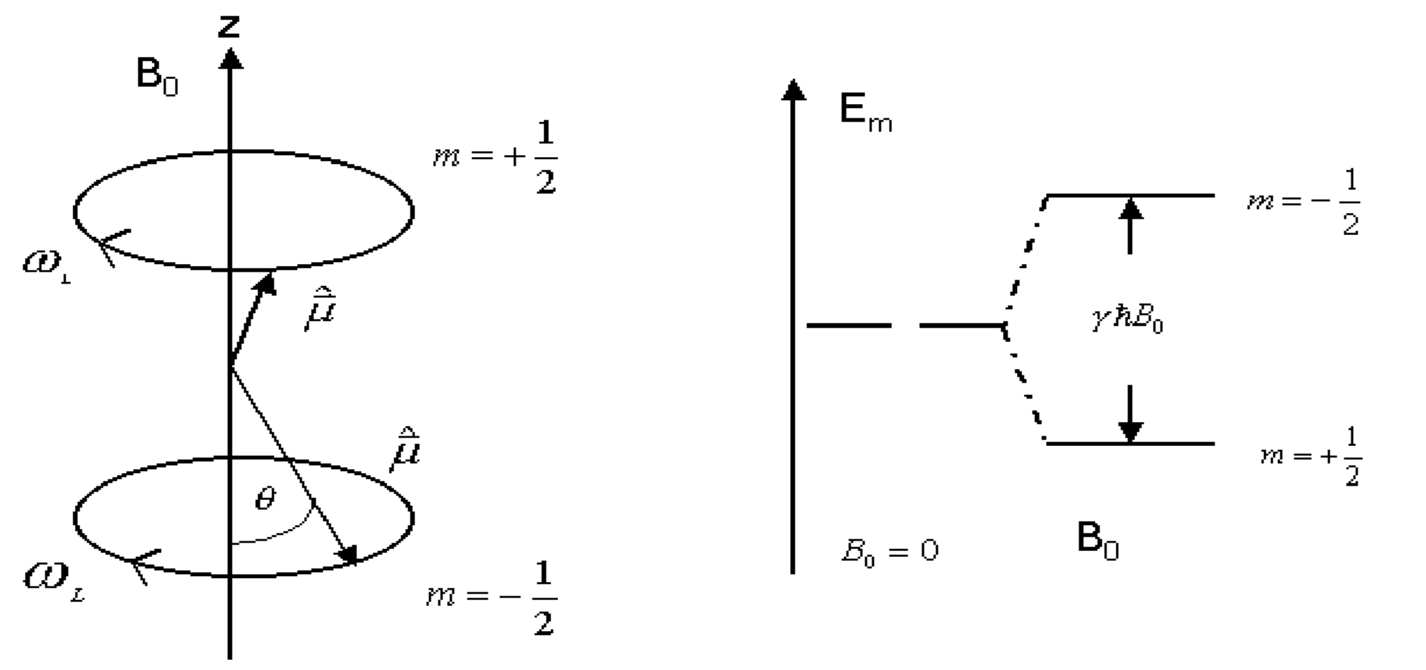

→ **NMR is element selective**

Precession

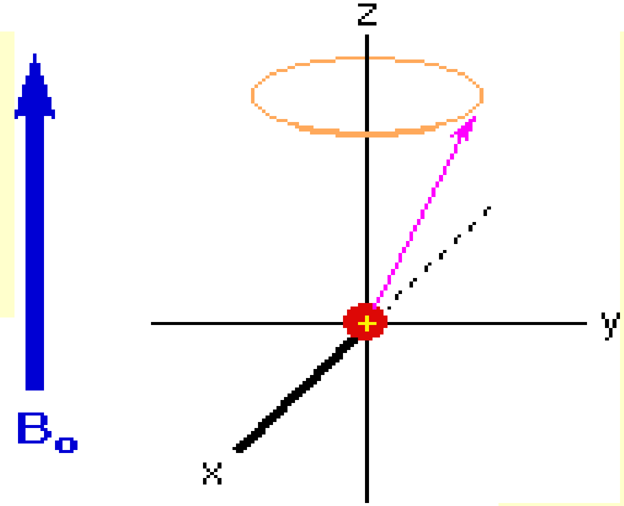

Precession of spins around external field similar to gyroscope

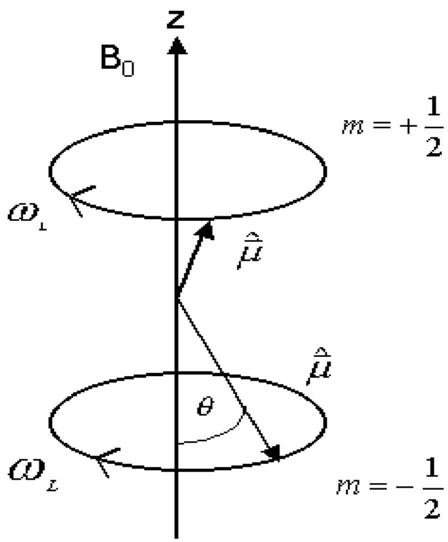

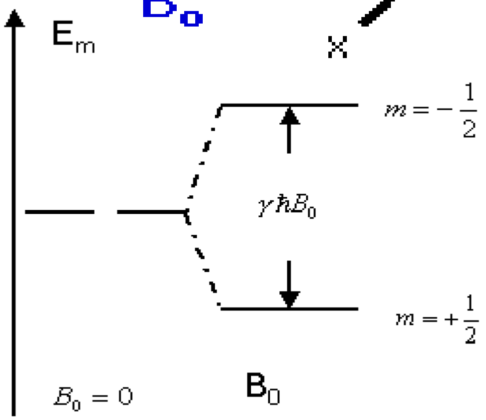

The precession (Larmor) frequency of the nuclei is given by

$$\omega_p = \gamma B_{eff}$$

where $B_{eff} = B_0 + B_{int}$

B_{int} contains important structural and chemical information

NMR measures the precession (Larmor) frequency

How is it done ?

By application of a second magnetic field fluctuating with frequency $\omega_o \sim \omega_p$

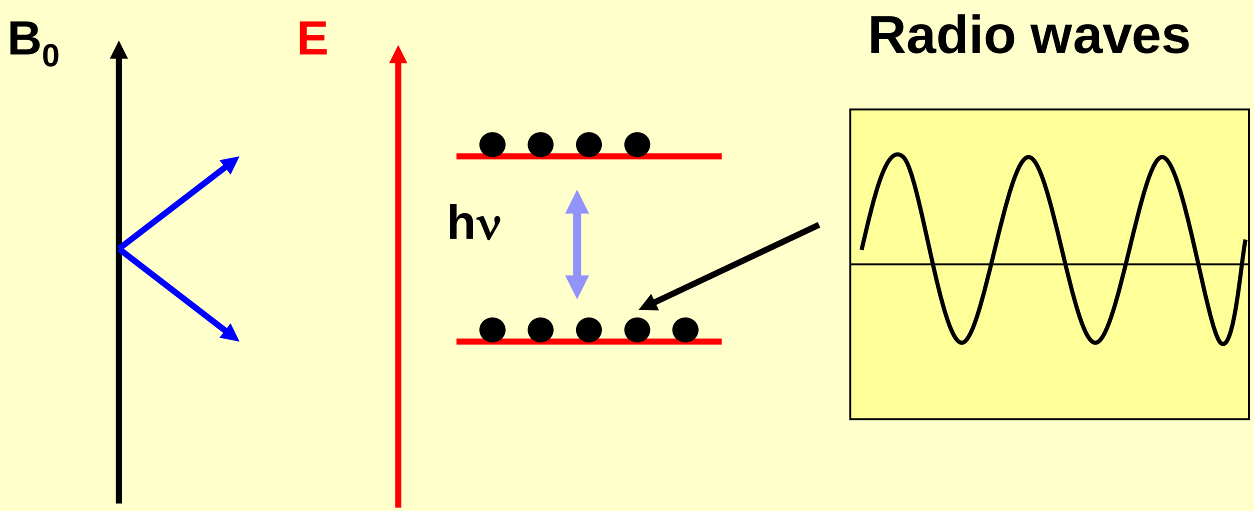

Resonance absorption occurs if $\omega_o \sim \omega_p$

Macro-sample: Boltzmann distribution ⇒ Magnetization

$$\mathbf{M_z} = \Sigma_i \frac{\mu_i}{V}\left(\frac{\mathrm{A}}{\mathrm{m}}\right)$$

Calculation of M_z:

$$E/V = \Sigma_i\, B_0\, n_i \mu_i / V = \quad M_z B_0$$

where: $\mu_i = m_i \gamma \hbar$ $n_i = \frac{\exp - E_i/k_BT}{\Sigma_i \exp - E_i/k_BT} N$

$$\exp - \frac{E_i}{k_BT} \approx 1 - \frac{E_i}{k_BT}$$

(HT approximation)

$E_i = - m_i \gamma \hbar B_0$

$\Sigma_i \exp - E_i/k_BT = 2I + 1$

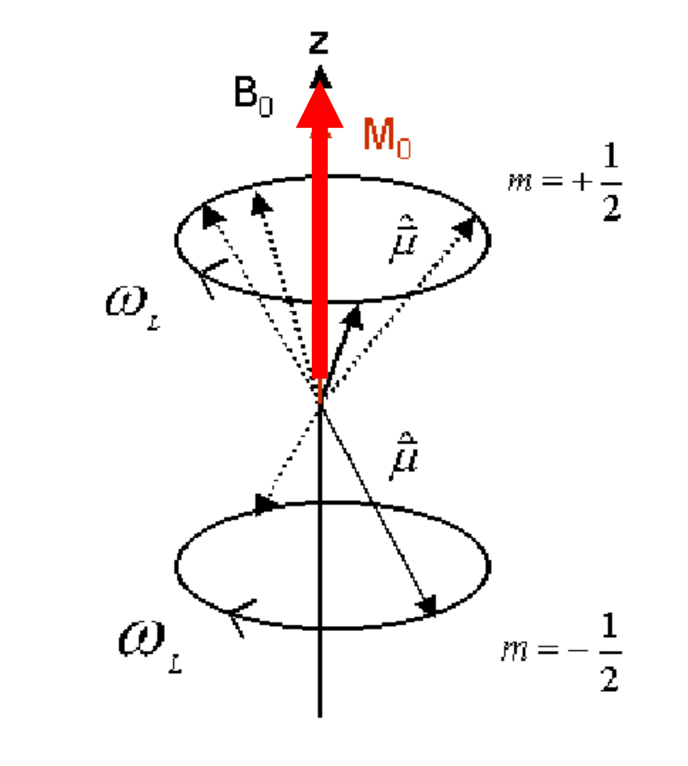

$$E/V = \Sigma_i \left(1 + \frac{m_i \gamma \hbar B_0}{k_BT}\right) m_i \gamma \hbar \frac{N}{V} \;=\; M_z B_0$$

Macroscopic magnetization in z-direction :

$$M_z = M_o = \frac{N/V\, \gamma^2 \hbar^2 I(I+1)}{3kT} B_o$$

No net magnetization in x- or y-direction

NMR is quantitative

Macroscopic Sample

In a sample spins are distributed among energy levels (Boltzmann-distribution)l

Macroscopic magnetization along B_0

No net magnetization in x- or y-direction

$$M_z = M_o = \frac{N/V\,\gamma^2 \hbar^2 I(I+1)}{3kT} B_o$$

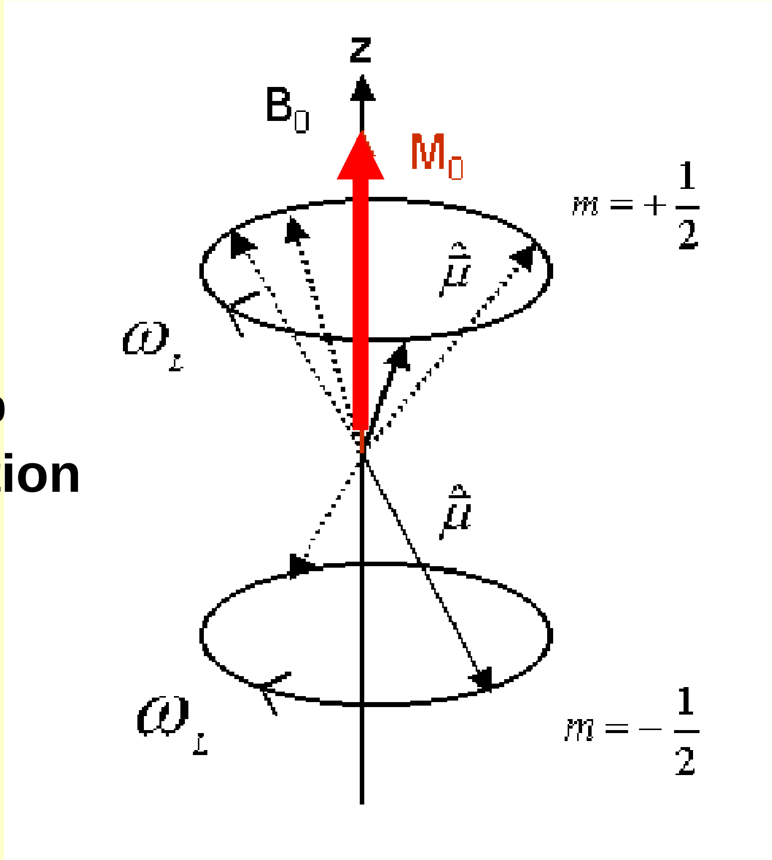

M_z is the source of the signal:
needs to be made time dependent to measure the precession frequency.

The Rotating Frame

In contrast to the B_0 field, the B_1 field changes direction in time with the frequency ω_0

To simplify the description of the magnetization's time dependence a rotating frame is introduced

Laboratory frame Rotating frame

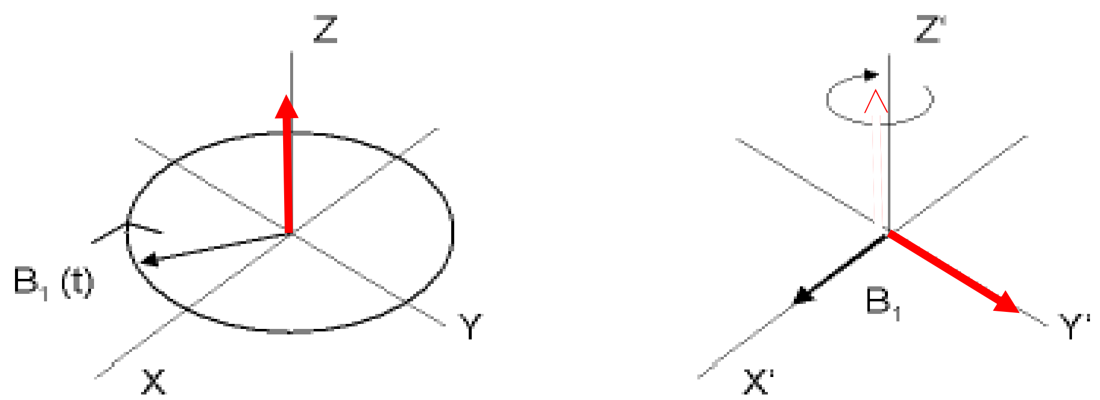

Rotating frame rotates with frequency ω_0 of B_1

90° pulse: rotates the z-magnetization into the x-y-plane
180° pulse: flips the z-magnetization into the –z-direction

Measuring NMR spectra

= Detection of Larmor frequencies present in the sample

1. B_1 field is irradiated for a short time t_p along the x,y direction
2. If $\gamma B_1 t_p = \pi/2$ then M_z is flipped by 90 degrees (90° pulse)
3. After the pulse, precession of M induces voltage in the coil.
4. This voltage, oscillating with ω_p, is the NMR signal

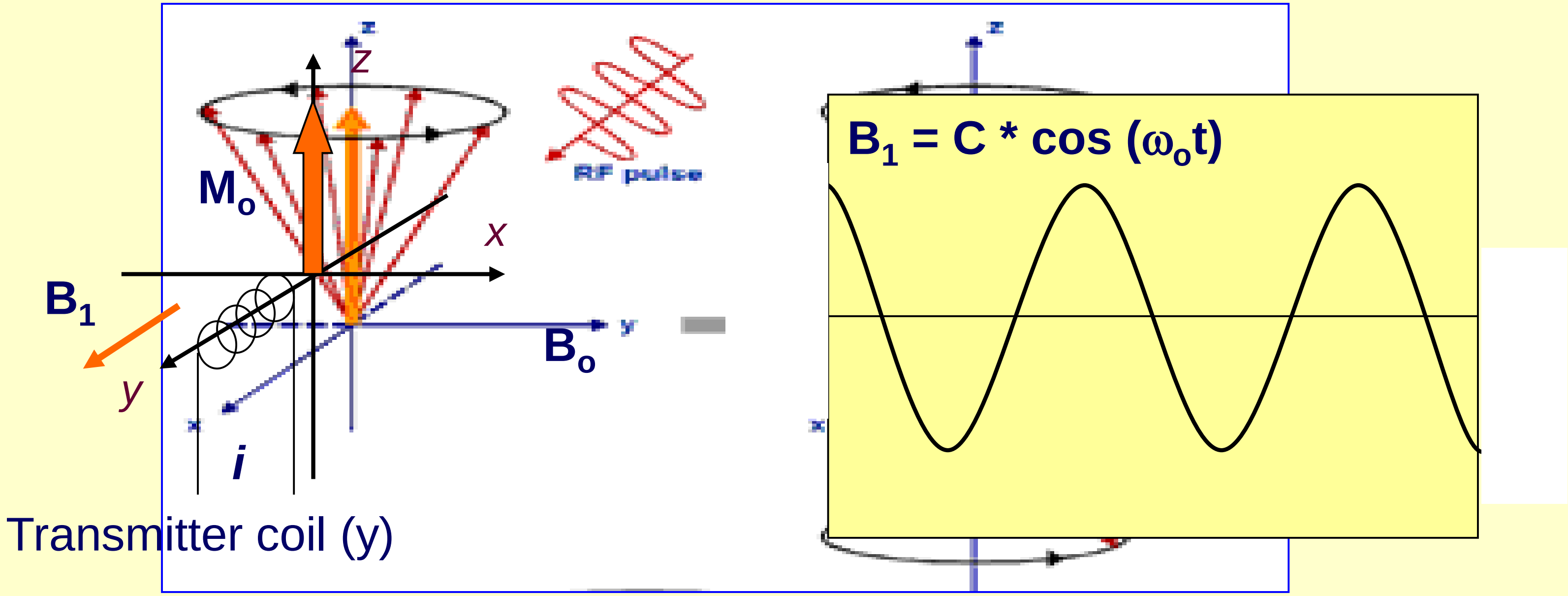

The Basic NMR Experiment

90° pulse -> magnetization flip

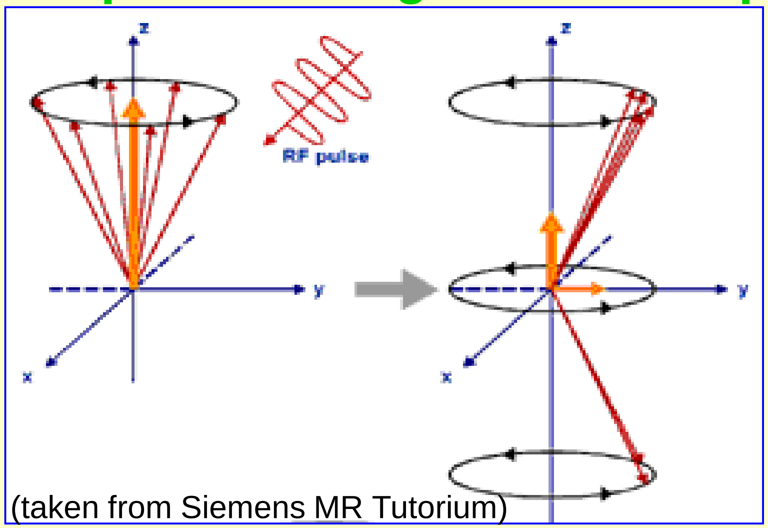

(taken from Siemens MR Tutorium)

Signal-

detection

Free Induction Decay

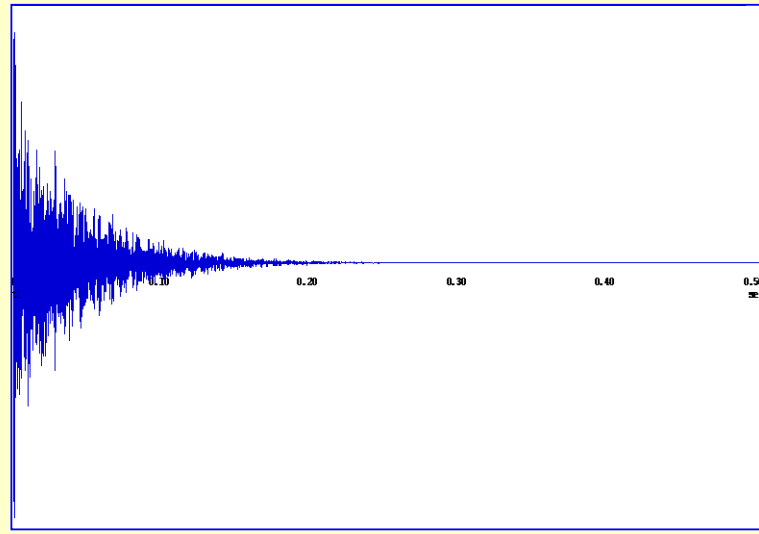

NMR-Spectrum

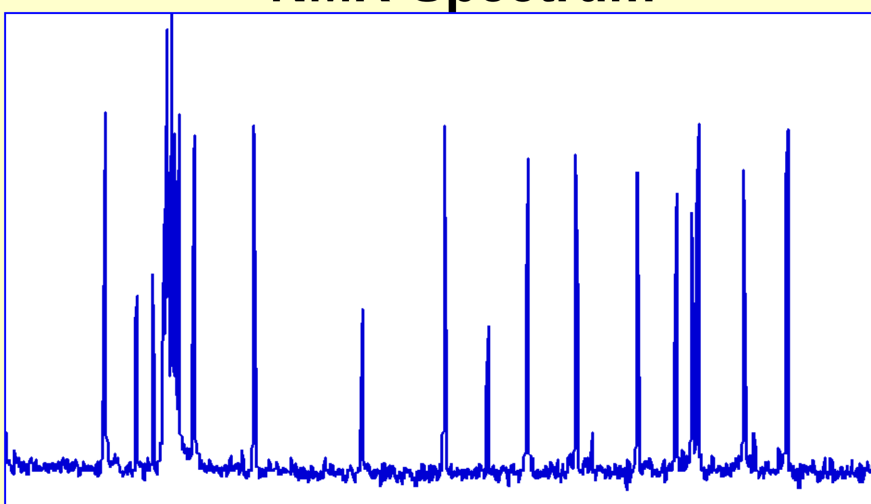

Fourier-Transformation

$$F(\omega) = \int_{-\infty}^{\infty} f(t) * e^{-i\omega t} dt$$

Schematic Experimental Set-up

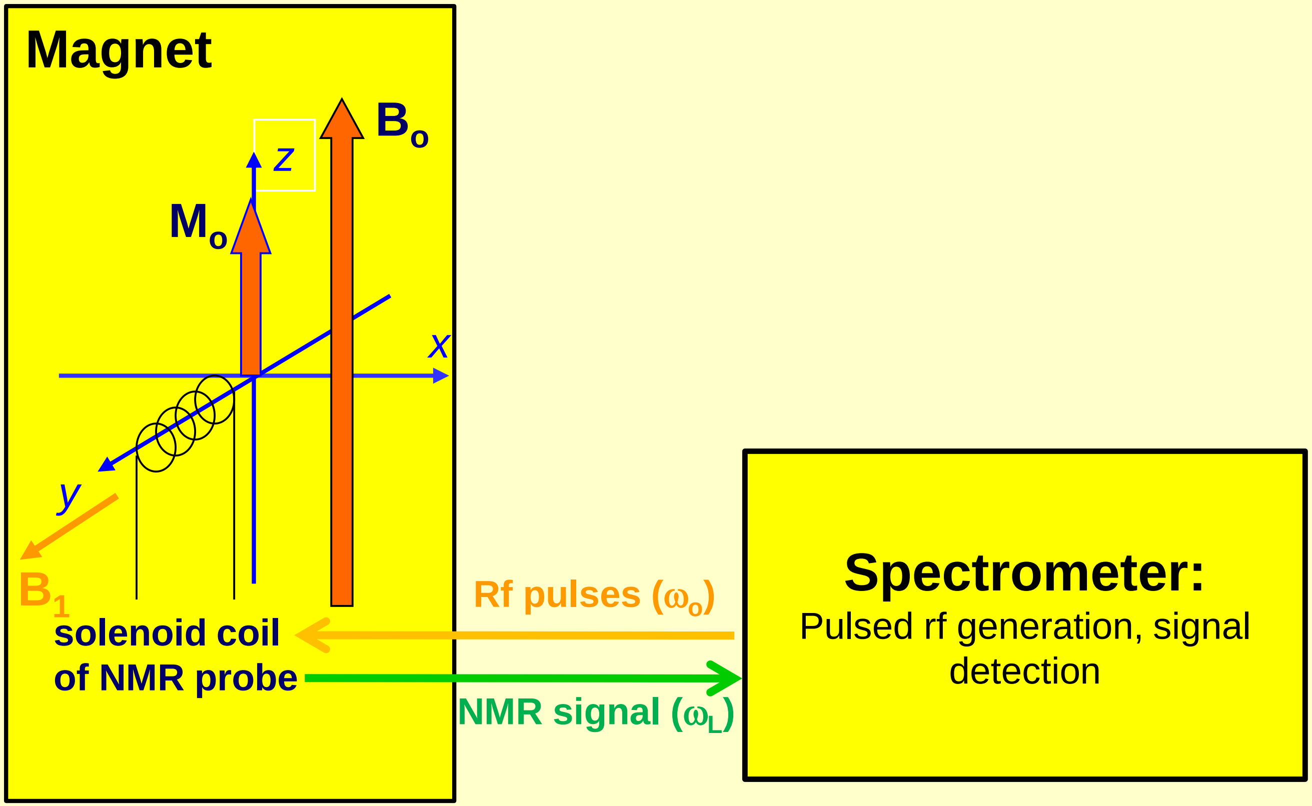

Equipment

magnet

probe

Sample in coil

Console:

signal excitation and detection

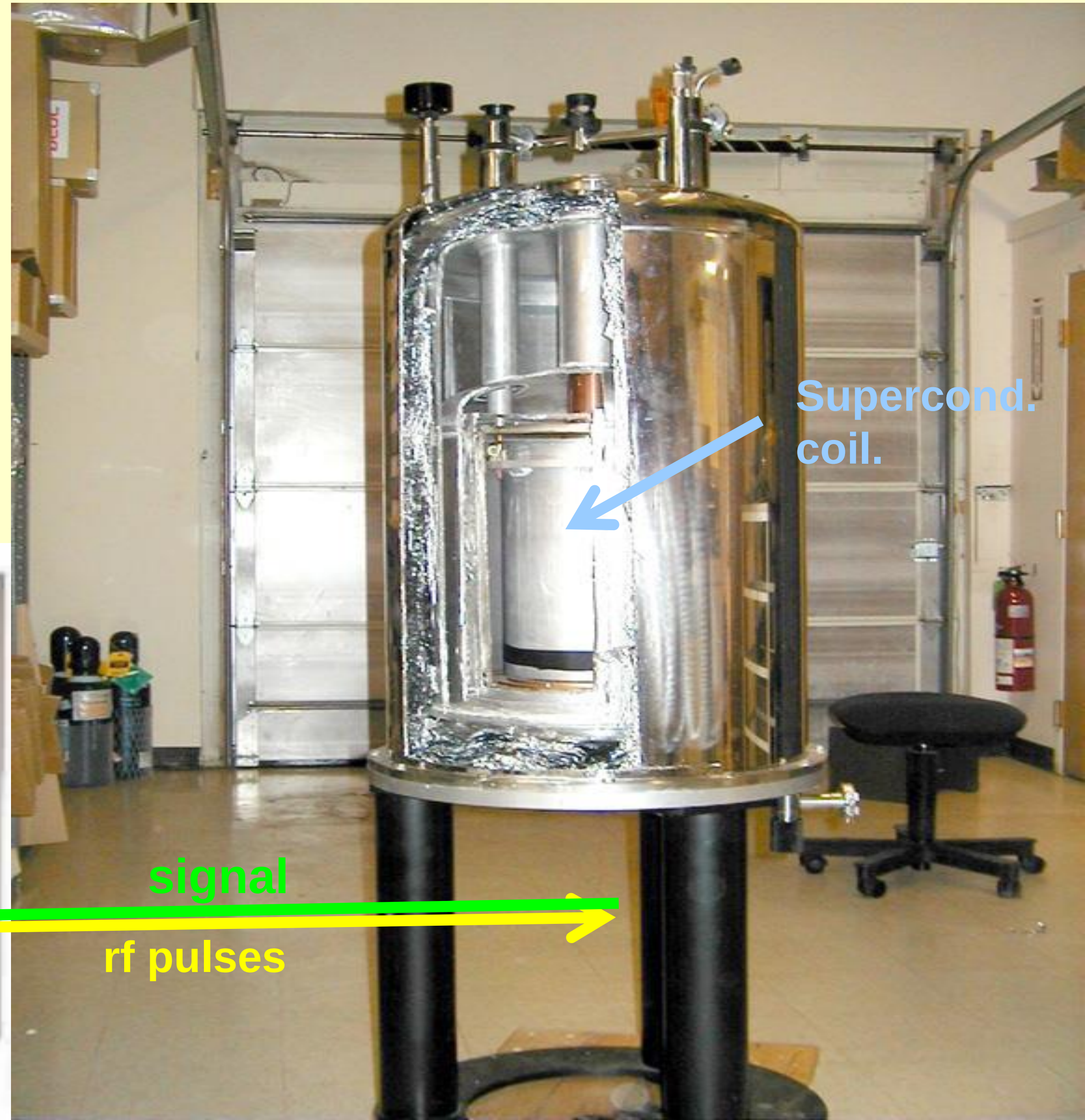

Relaxation Processes

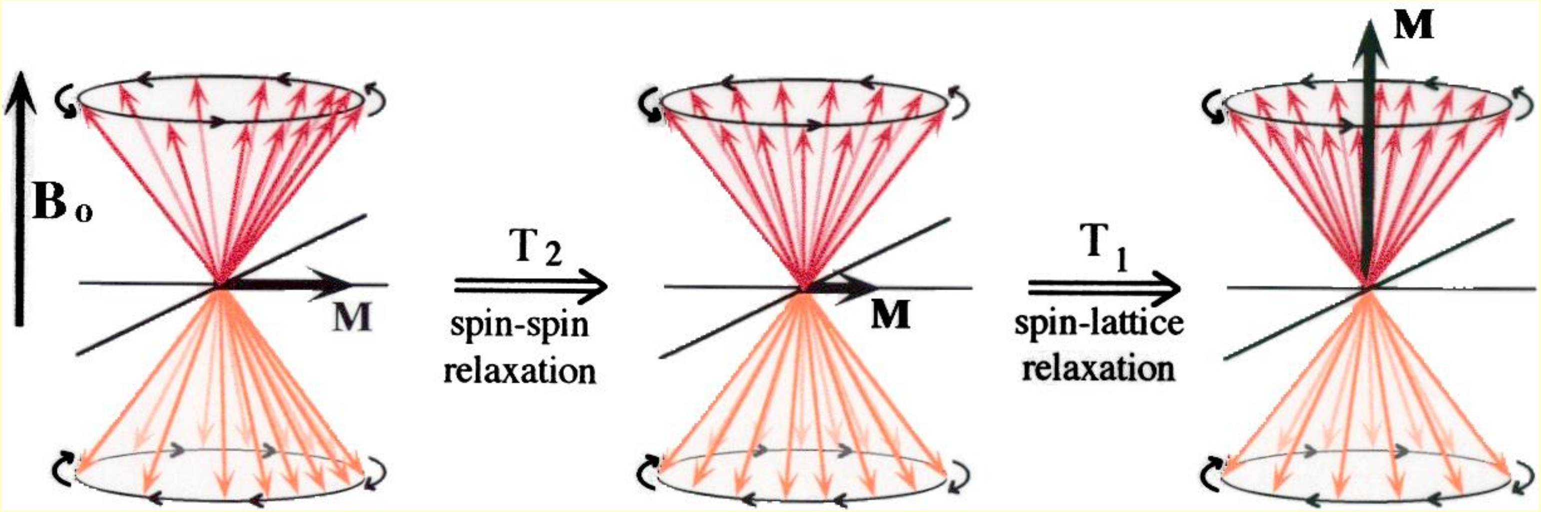

Transverse relaxation (T_2): dephasing of spins in the x-y plane (distribution of precession frequencies, spin-spin interactions)

Longitudinal relaxation (T_1): build-up of z-magnetization (return to equilibrium, energy exchange with surroundings (lattice)

Spatial distribution models in glasses

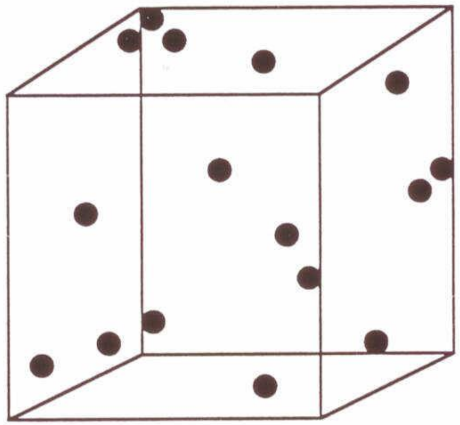

random

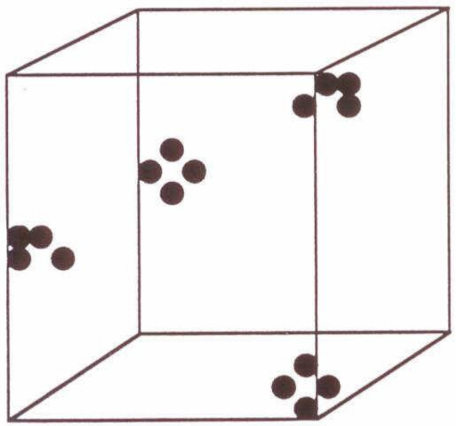

clustered

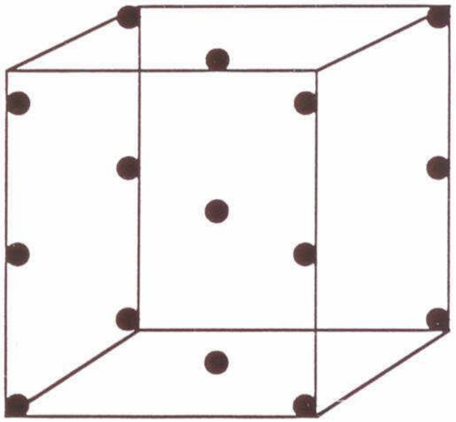

uniform

Selective measurement by spin-echo decay

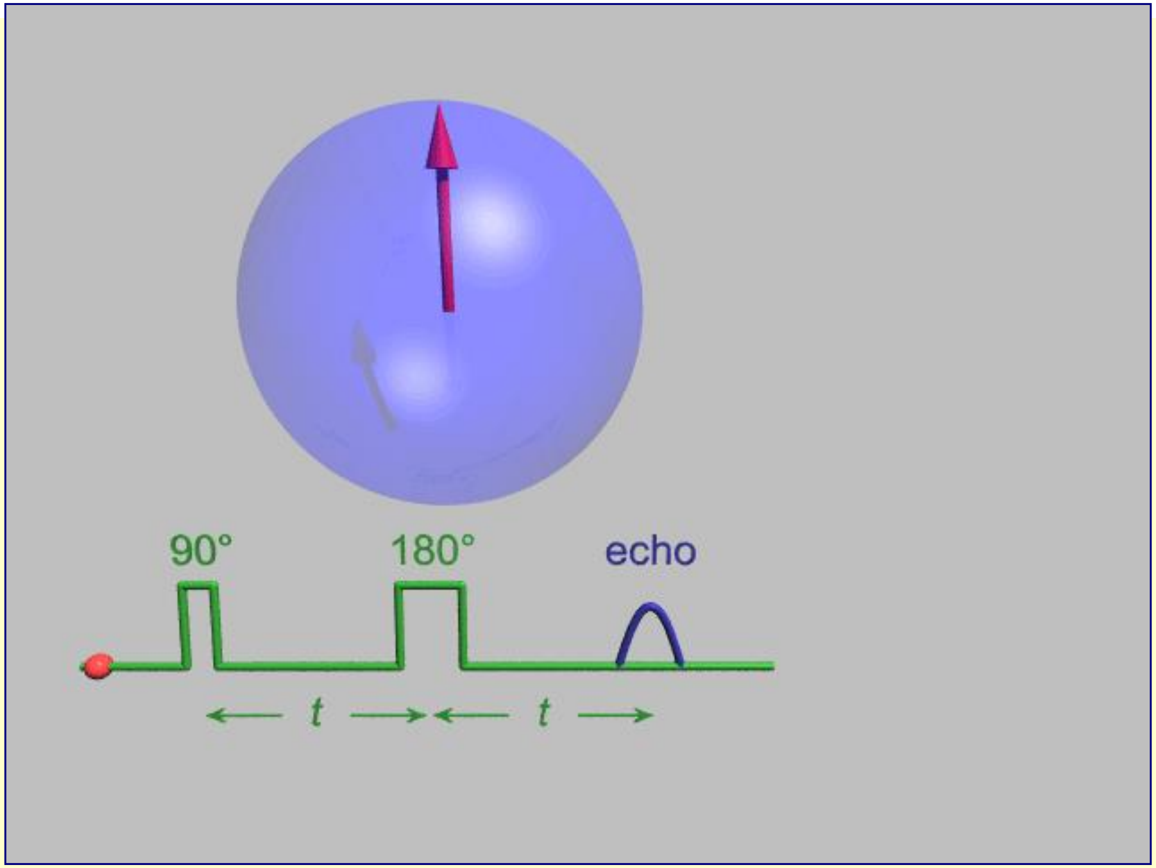

Selective for homonuclear dipole coupling strengths

$$S/S_0 = \exp - (2t^2 M_2)$$

Four distinct interactions

- magnetic shielding
- Electric quadrupole coupling
- Indirect spin-spin coupling
- magnetic dipole coupling

In the solid state:

anisotropy: $\omega_p \sim 3\cos^2\theta - 1$

Magnetic Shielding

Resonance frequency (bare nucleus): $\omega_0 = \gamma B_0$

Effective magnetic field at nucleus: $B_{eff} = B_0(1-\sigma)$

Resonance frequency (real sample) $\omega_L = \gamma B_0(1-\sigma)$

Chemical shift

$$\delta \equiv \frac{\omega_L^x - \omega_L^{ref}}{\omega_L^{ref}}$$

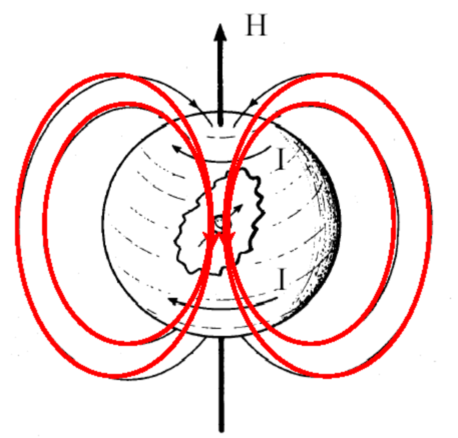

Effective magnetic field arises from shielding or deshielding of the external magnetic field by electrons

Probe for electronic environment (bonding)

Chemical Shielding Anisotropy

Solid state : chemical shielding is anisotropic:
➔ tensorial description

$$\omega_L = \omega_0 \left[1 - \sigma_{iso} - \frac{1}{3}(\sigma_{z'z'} - \sigma_{x'x'})(3\cos^2\theta - 1) \right]$$

powdered sample

Distribution of orientations

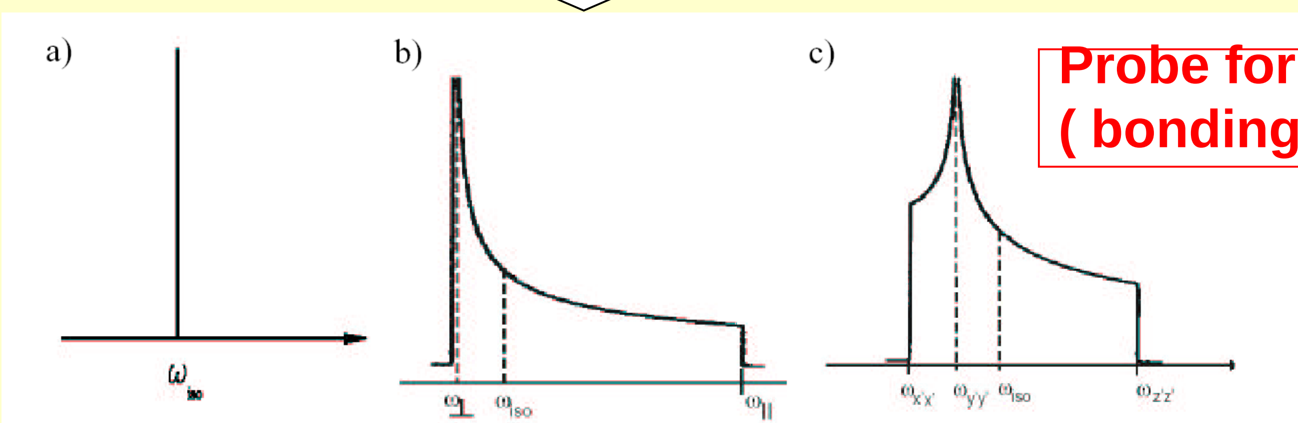

Probe for local symmetry (bonding geometry)

cubic **Axially symmetric** **Asymmetric**

Example : ^{31}P NMR of Phosphates

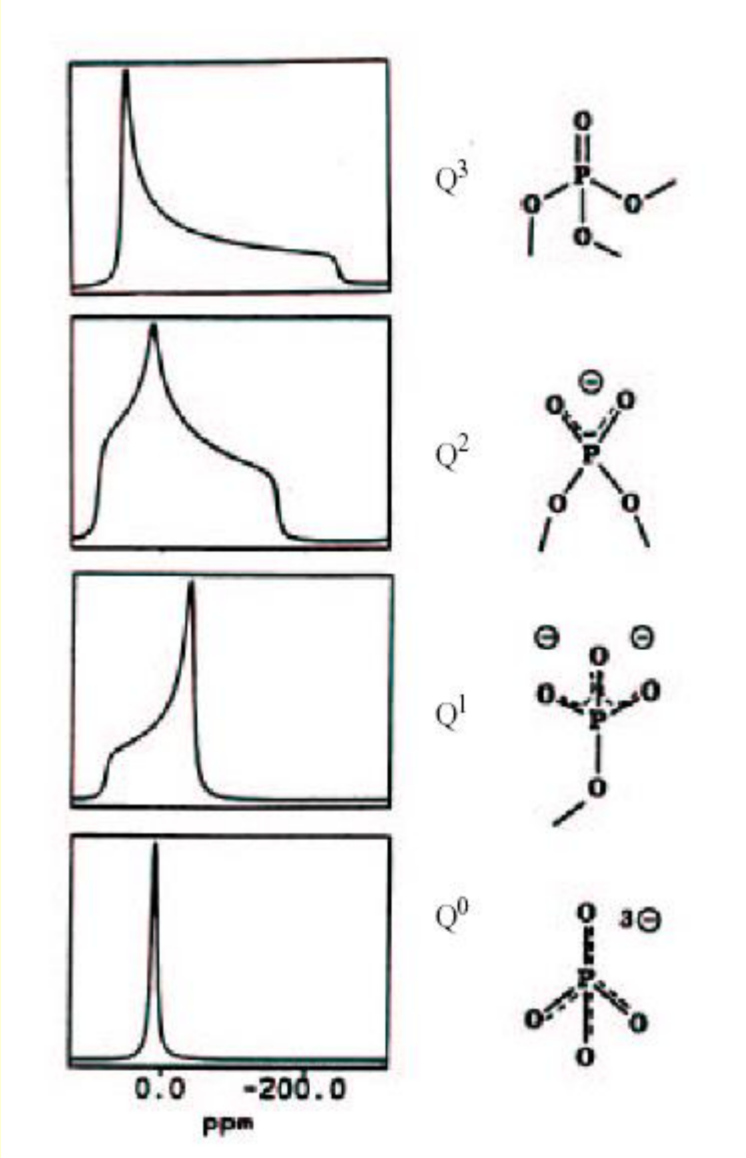

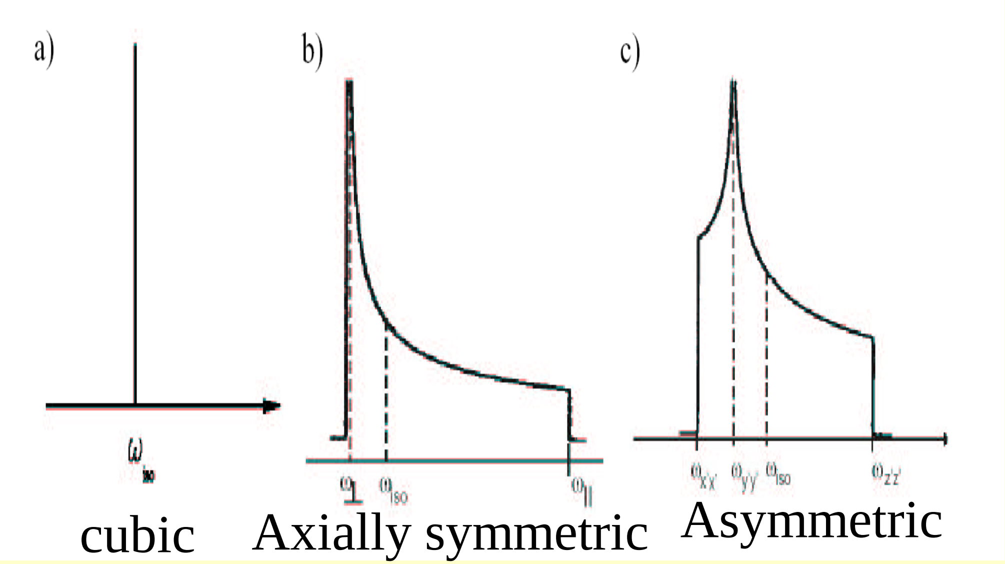

Indirect spin-spin Coupling

- Spin-spin interaction transmitted via polarization of bonding electrons
- HAMILTONIAN $\mathcal{H}_J = 2\pi\, \hat{\mathbf{I}}_1\, \mathbf{\mathfrak{J}}\, \hat{\mathbf{I}}_2$ homonuclear
- $\mathcal{H}_J = 2\pi\, \hat{\mathbf{I}}\, \mathbf{\mathfrak{J}}\, \hat{\mathbf{S}}$ heteronuclear
- Anisotropy accounted for by tensorial description
- Isotropic component: $\mathbf{J}_{iso}$ (scalar, isotropic coupling constant)
- Anisotropic component: $\Delta\mathbf{J}$, same dependence on spin operators as the through-space dipole-dipole coupling
- Liquid-state and MAS-NMR: only $\mathbf{J}_{iso}$ relevant: $\Pi_i\, (2n_i I_i + 1)$ multiplicity rule
- n_i = number of equivalent spins of quantum number I_i the observed nucleus is coupled to

Mechanism: Spin polarization of bonding electrons

One bond: $^{1}J > 0$

Observe nucleus

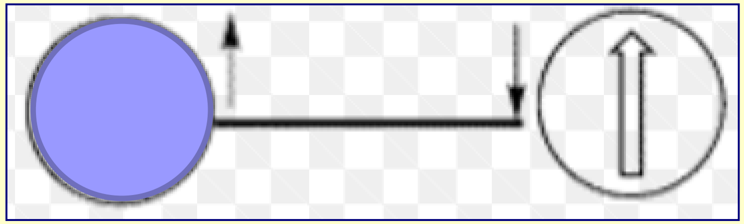

Perturbing Nucleus, m =1/2

Observe nucleus

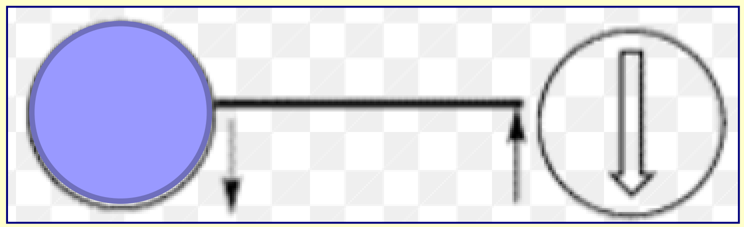

Perturbing Nucleus, m = -1/2

Two bonds: $^{2}J < 0$

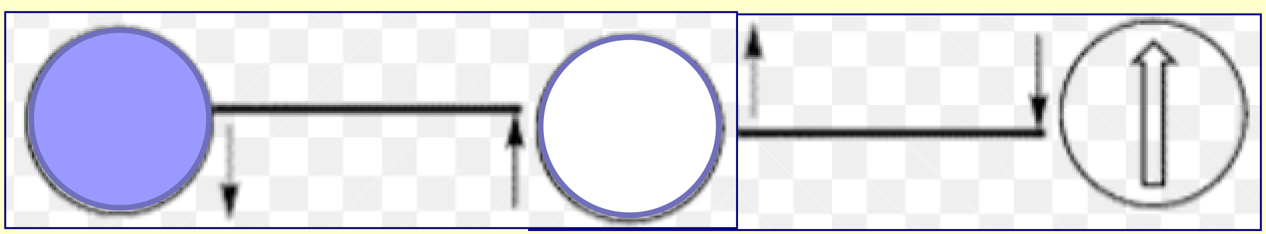

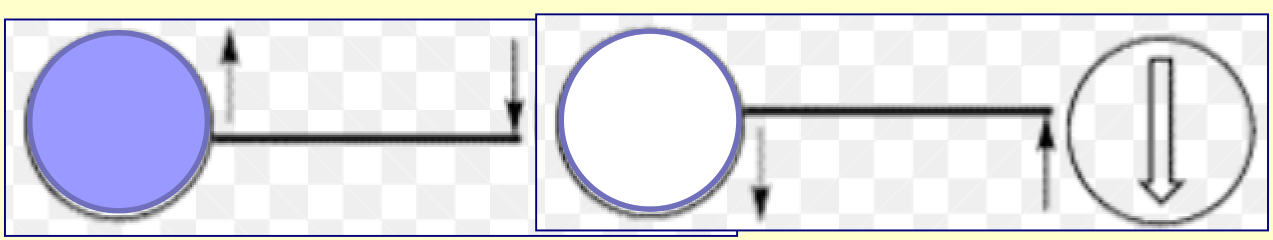

Three bonds: $^3J > 0$

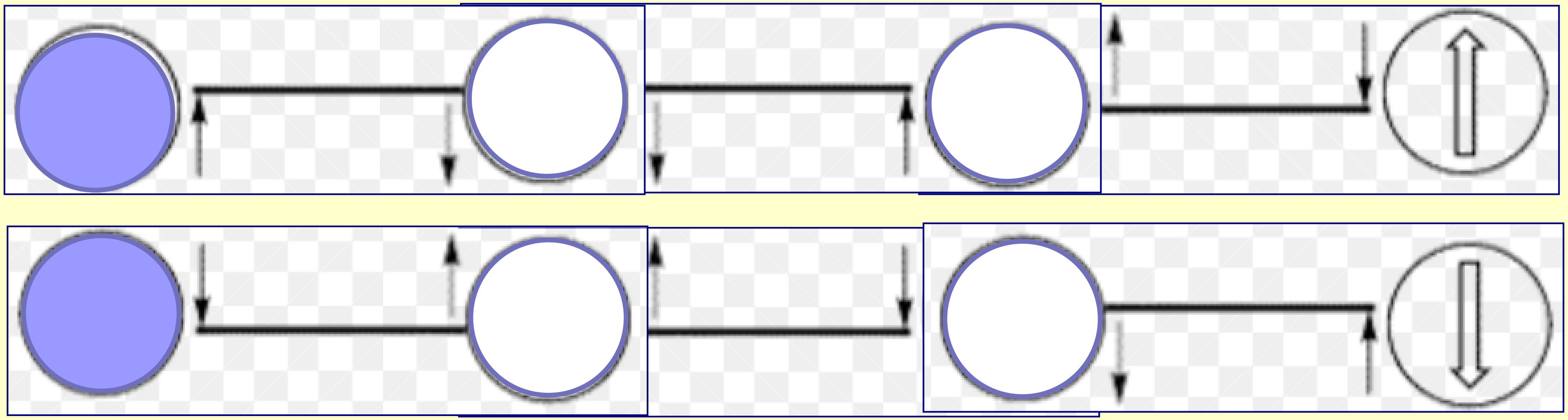

^1H NMR spectrum of ethanol

1

1 1

1 2 1

1 3 3 1

1 4 6 4 1

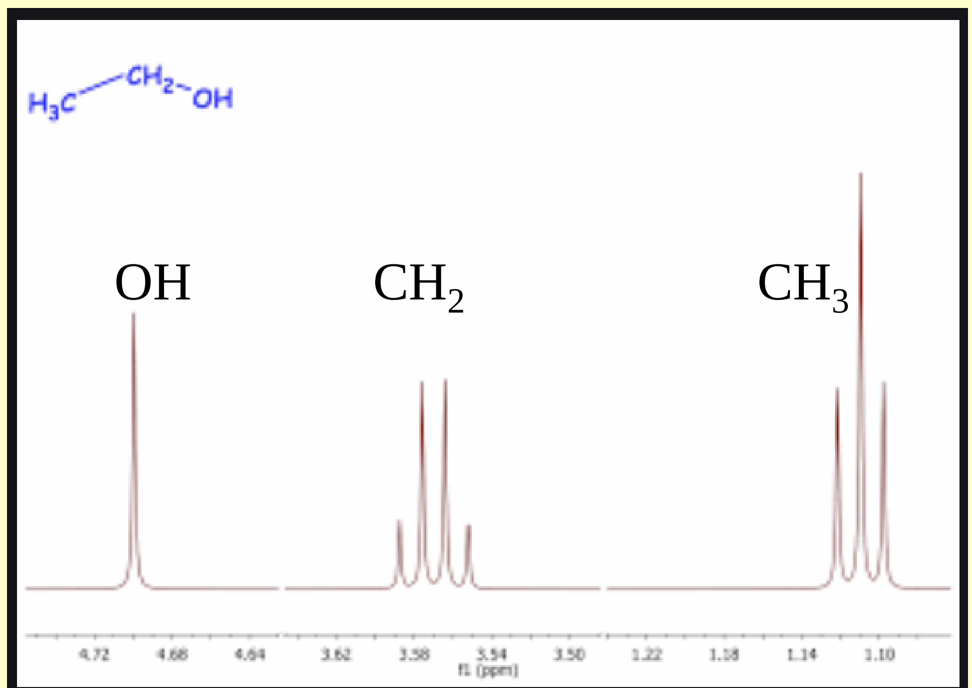

Examples of Spin-Spin Coupling Multiplicities

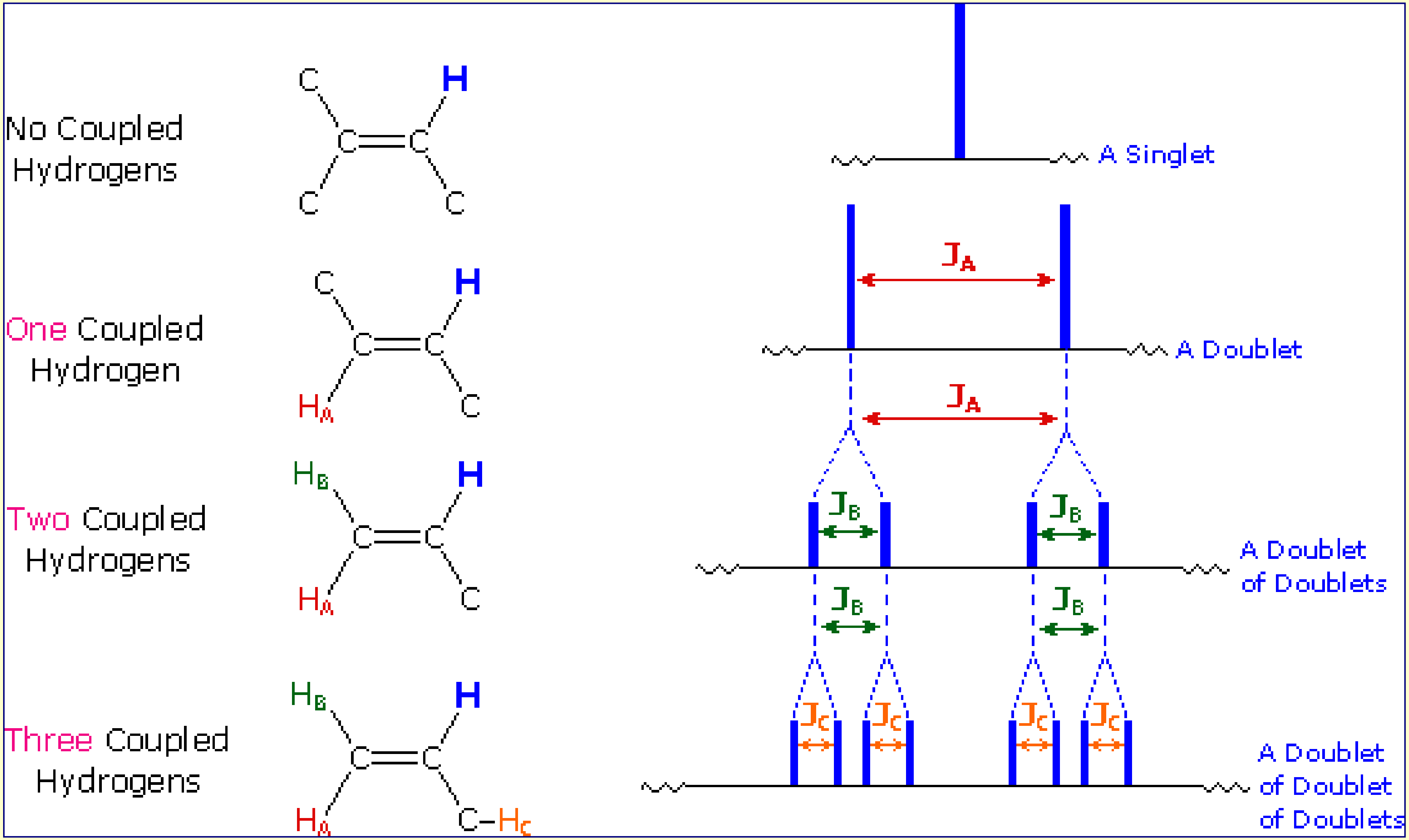

Karplus-Relation for J-coupling

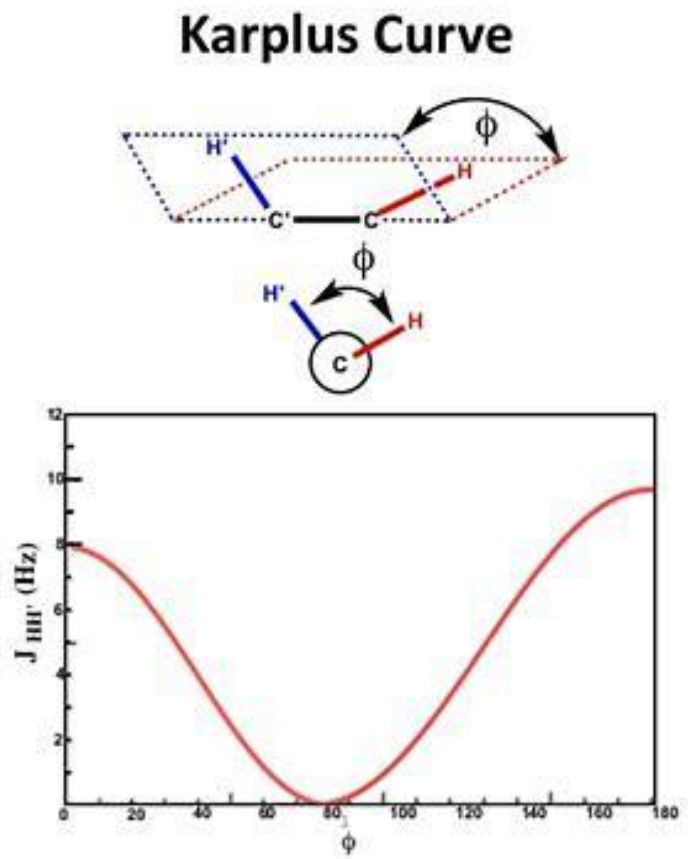

For ^3J (^1H-^1H) coupling:

$$J(\phi) = C\cos 2\phi + B\cos\phi + A$$

A **= 4.22,** ***B*** **= −0.5, and** ***C*** **= 4.5 Hz.**

Important for conformational studies (protein folding)

Nobel Prize 2013

MAS conditions: isotropic peak splitting

^{31}P MAS-NMR of $(CuI)_3P_4S_4$

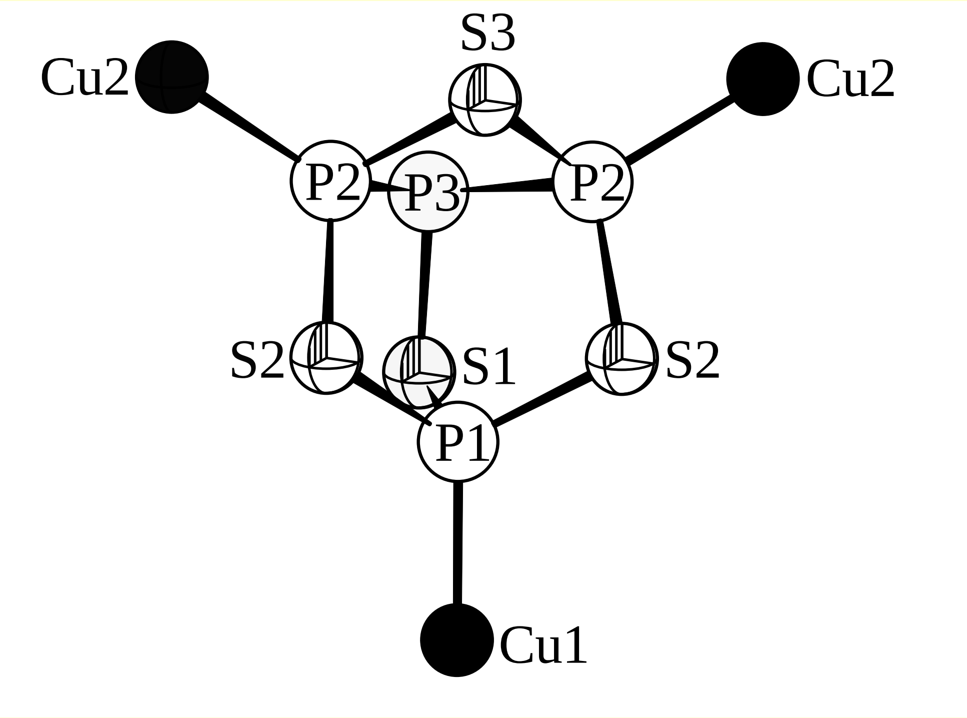

Proof of connectivity P-Cu

^{63,65}Cu: I =3/2

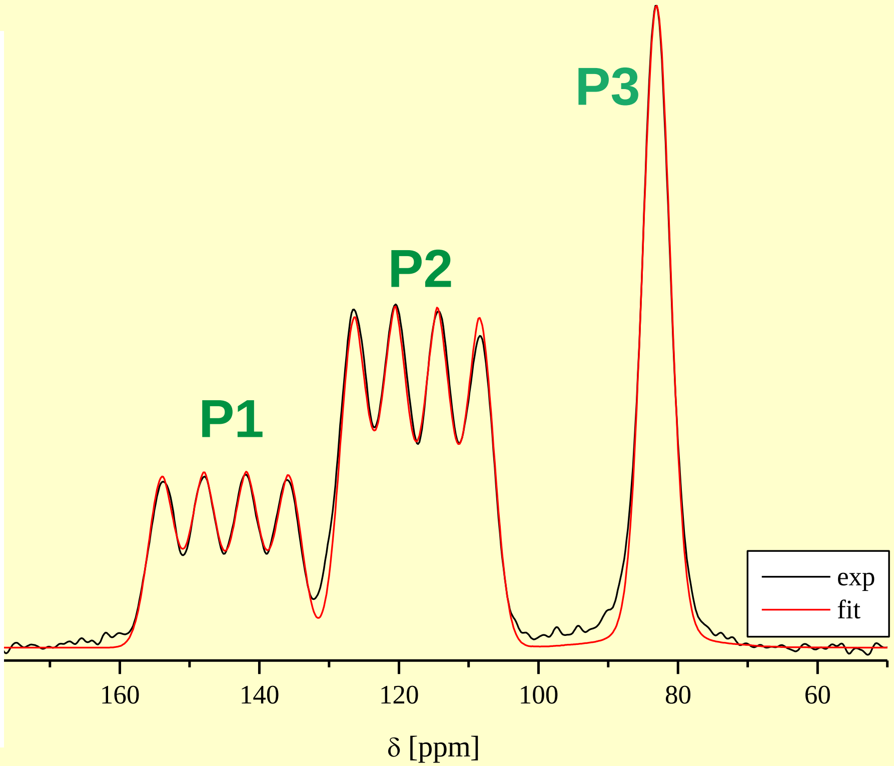

G. Brunklaus, J. C.C. Chan, H. Eckert, S. Reiser, T. Nilges, A. Pfitzner, Phys. Chem. Chem. Phys. 5, 3678 (2003)

Magnetic dipole interactions

Magnetic moments of nearby spins affect the local magnetic field and thus the resonance frequency. „Through-space“ interaction

$$\hat{H}_{DIP}(ij) = -\frac{\mu_0}{4\pi}\gamma_i\gamma_j\hbar^2 r_{ij}^{-3}\left[\hat{A} + \hat{B} + \hat{C} + \hat{D} + \hat{E} + \hat{F}\right]$$

Probe of internuclear distance

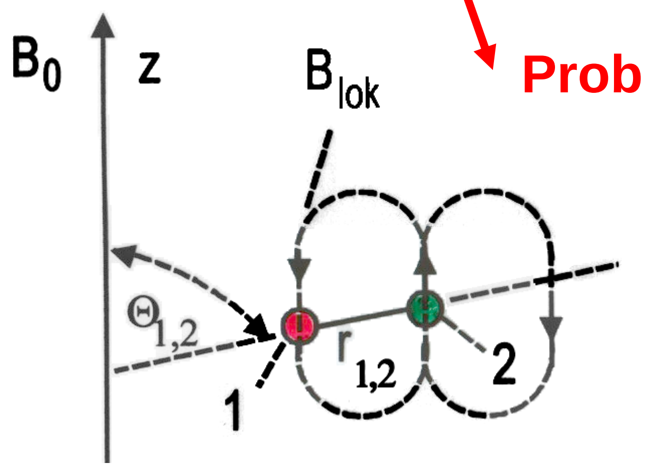

$\hat{A} \sim (\hat{I}_{z1}\hat{I}_{z2})\,(3\cos^2\Theta - 1)$ **homo- & heteronuclear**

$B \sim (\hat{I}^+_1\hat{I}^-_2 + I^-_1 I^+_2)\,(3\cos^2\Theta - 1)$ **only homonuclear**

Dipolar Hamiltonian Terms

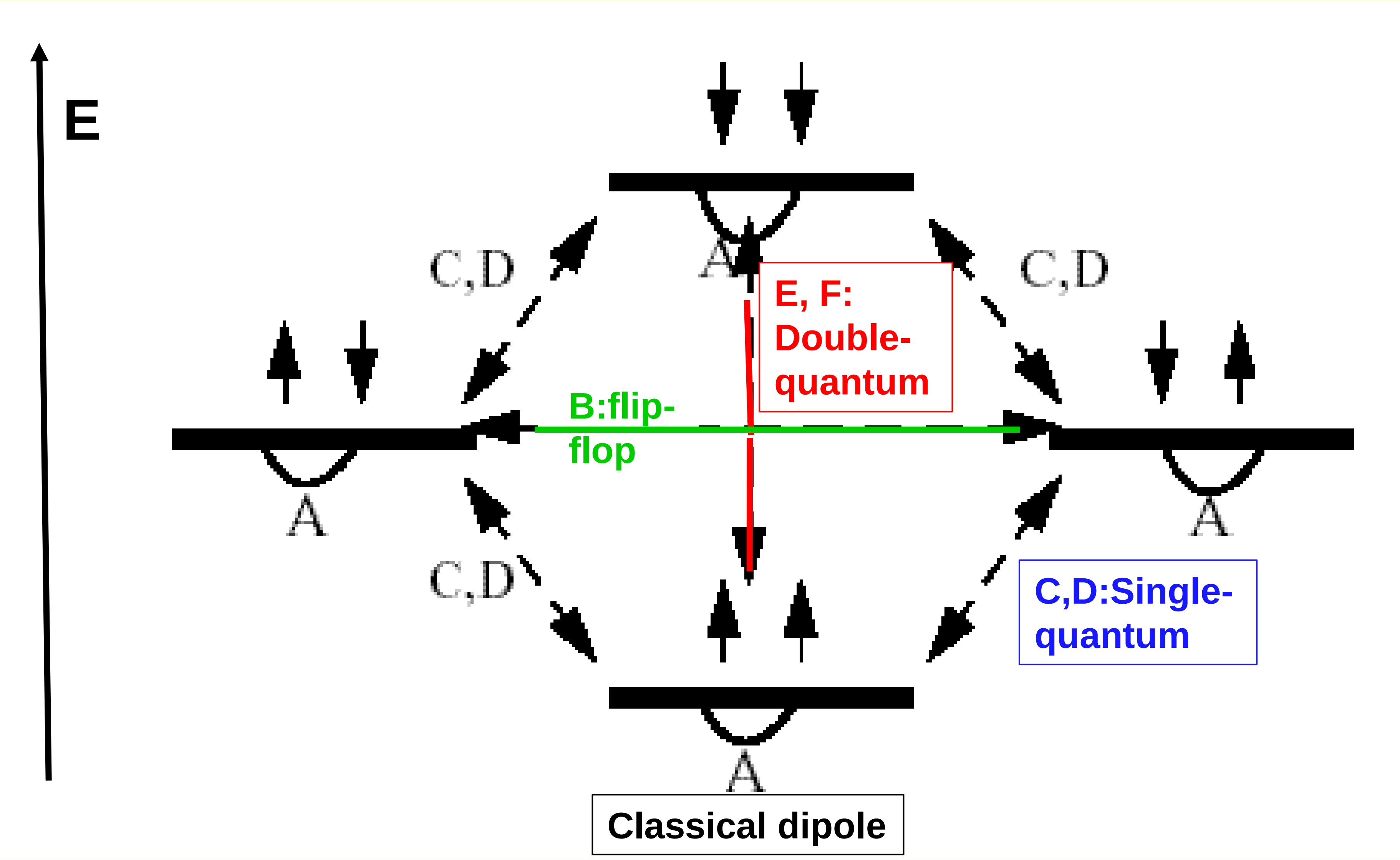

Lineshape of a two-spin system

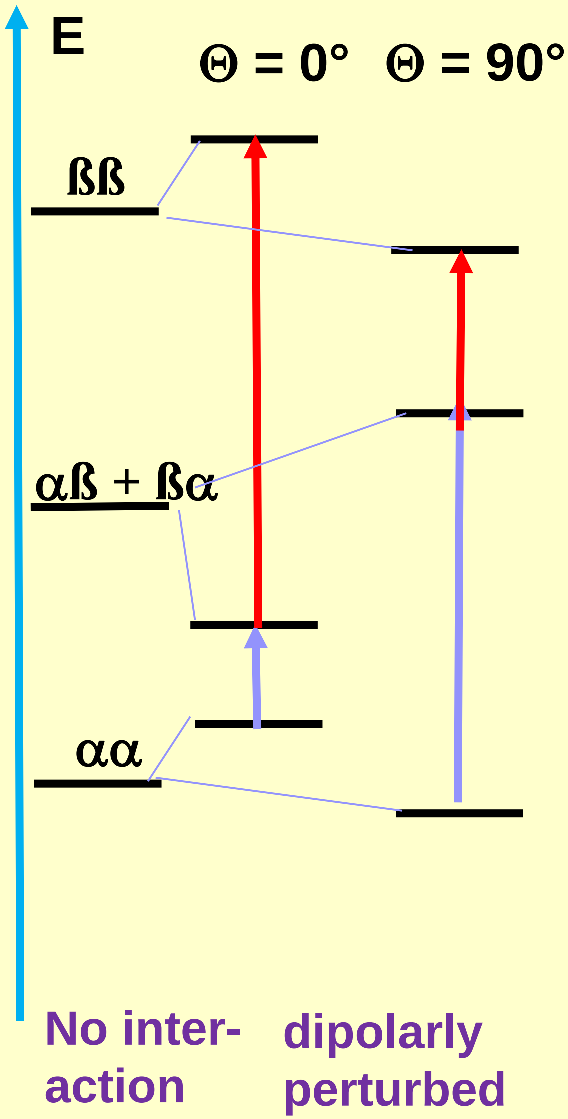

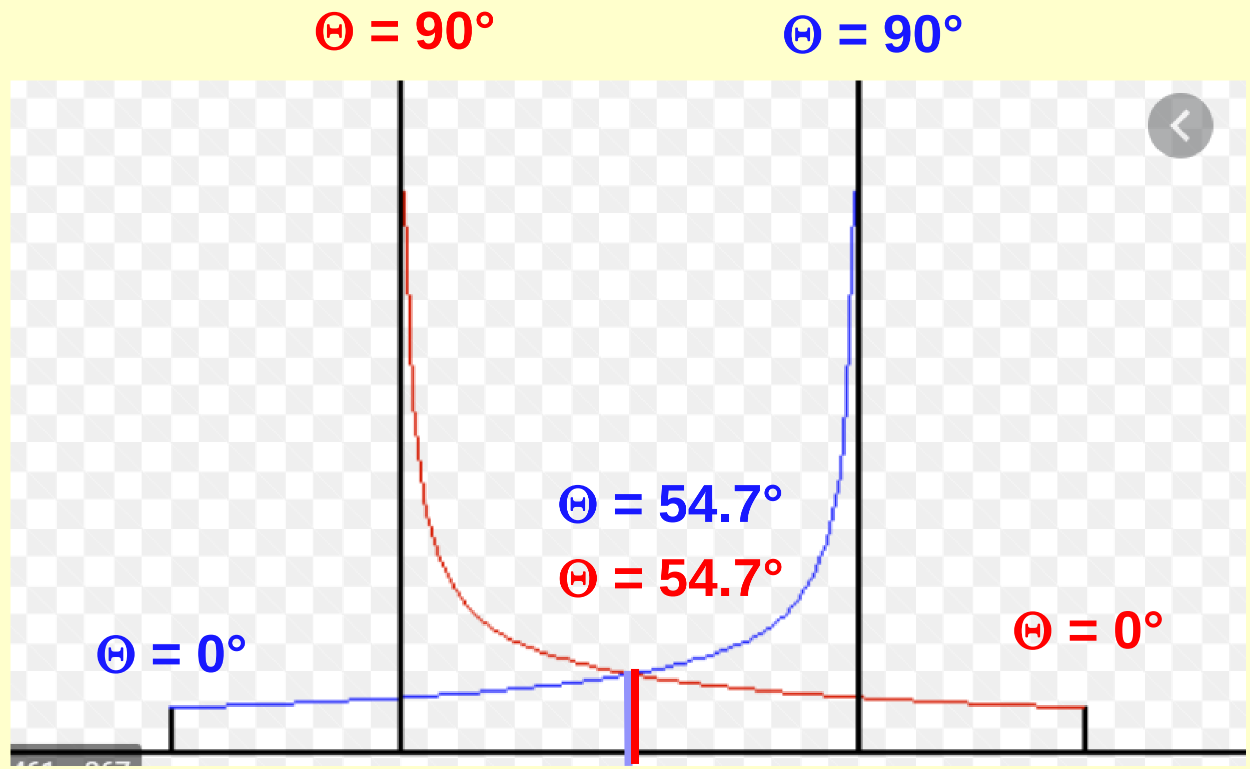

„Pake Doublet“:
Superposition of two powder patterns

Peak splitting $(\mu_0/4\pi)\gamma_1\gamma_2 h^2(3\cos^2\Theta-1)/r^3$

In the liquid state and under MAS conditions: dipole coupling averaged to zero

Second Moment Description of Multi-Spin Interactions

Specification of an average dipolar coupling in multi-spin systems Where details of the spin geometry are not well known. Using this method distance scenarios can be tested

Definition:

Time domain:
Curvature of f(t) at origin

$$f(t) = f(0)\left\{ 1 - M_2 t^2/2! + M_4 t^4/4! - .... \right\}$$

$$M_2 = - f(0)^{-1}\left\{ d^2 f(t)/dt^2 \right\}_{t=0}$$

Frequency domain:
std. deviation of frequency

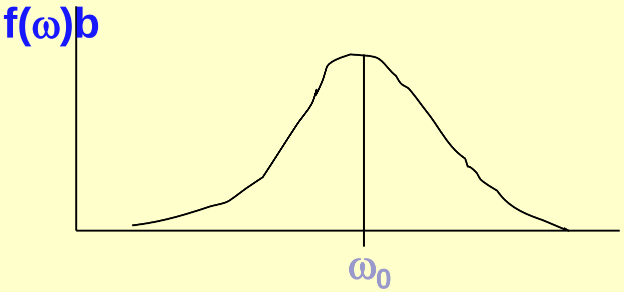

$$M_2 = \frac{\int (\omega - \omega_0)^2 f(\omega) d\omega}{\int f(\omega) d\omega}$$

Relation to structure:

$$M_2 = \frac{4}{15}\left(\frac{\mu_0}{4\pi}\right)^2 \gamma_I^2 \gamma_S^2 \hbar^2 S(S+1) \sum \frac{1}{r_{ij}^6} \quad \text{(hetero)}$$

$$M_2 = \frac{3}{5}\left(\frac{\mu_0}{4\pi}\right)^2 \gamma^4 \hbar^2 I(I+1) \sum \frac{1}{r_{ij}^6} \quad \text{(homo)}$$

$$\sum \frac{1}{r_{ij}^6}:$$

Convergence at 4 times the shortest distance

Spatial distribution models in glasses

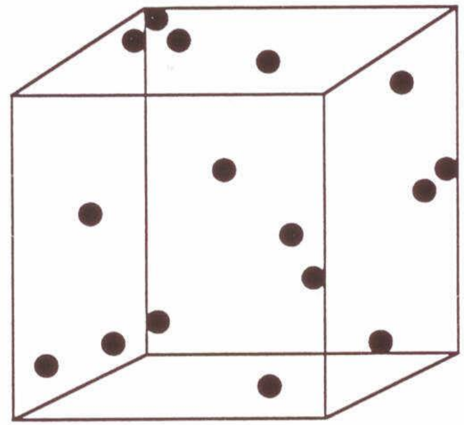

random

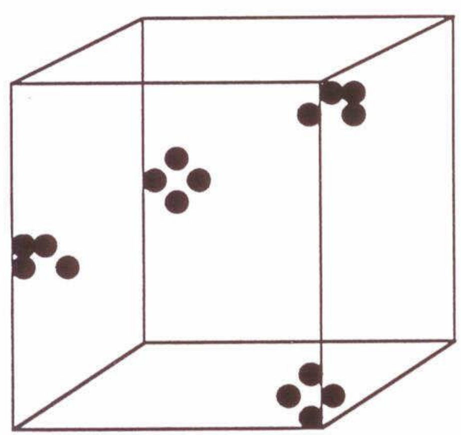

clustered

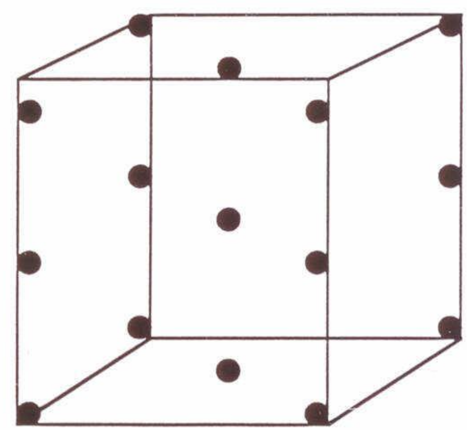

uniform

Selective measurement by spin-echo decay

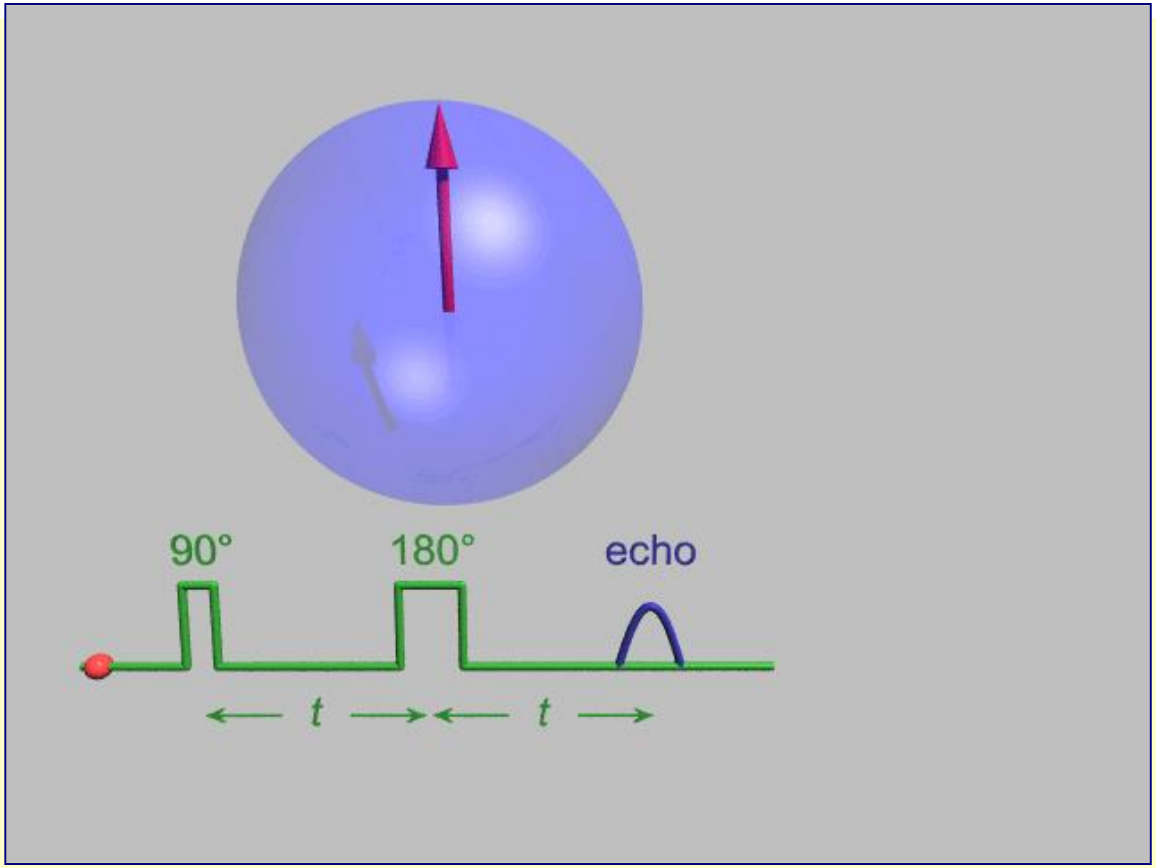

Selective for homonuclear dipole coupling strengths

$$S/S_0 = \exp - (2t^2 M_2)$$

Spatial Atomic Distributions in P-Se Glasses

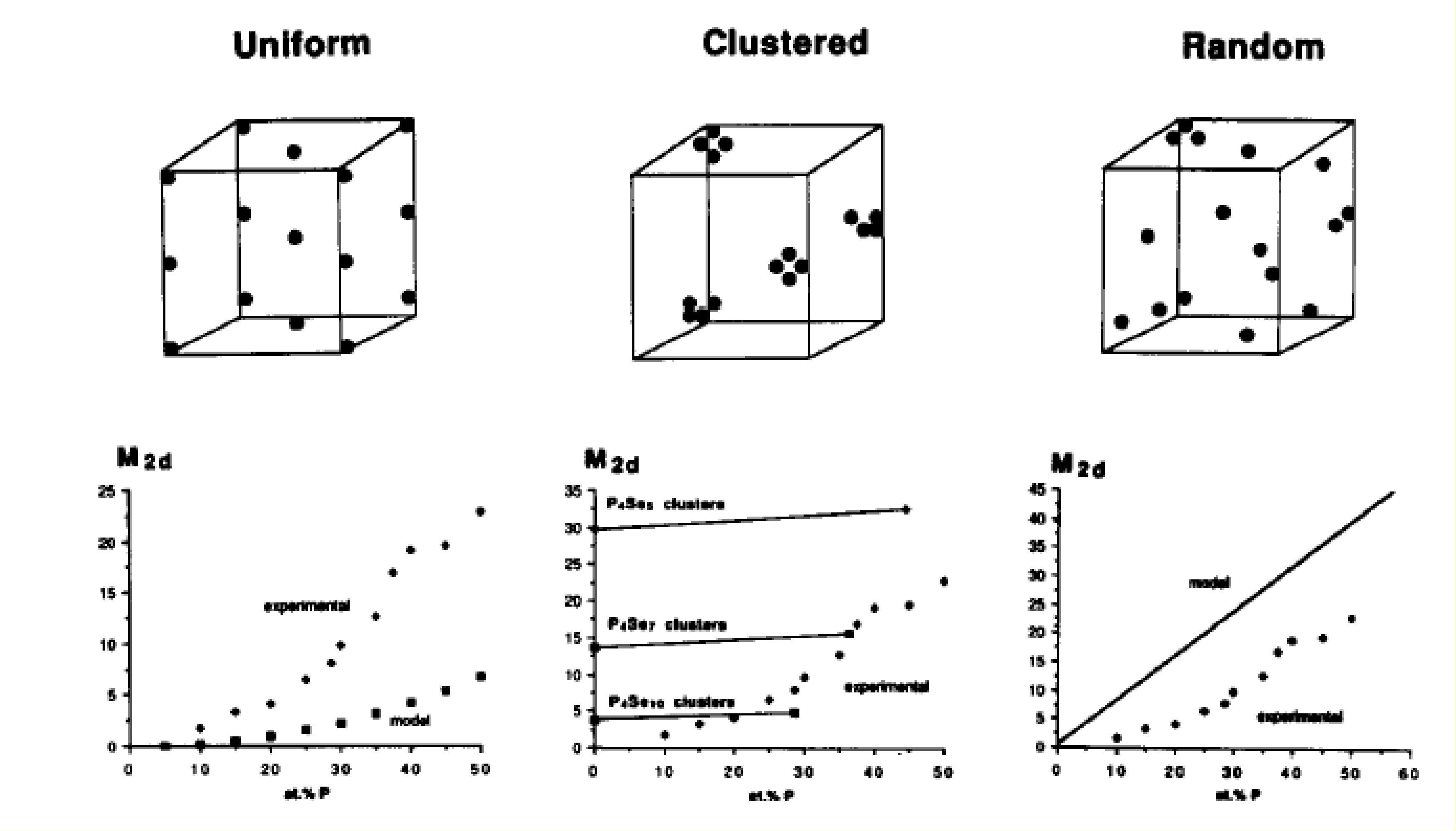

P-Se vs. P-P- bonding

D. Lathrop, H. Eckert, J. Am. Chem. Soc. 111 (1989), 3536

D. Lathrop, H. Eckert, Phys. Rev. B 43 (1991), 7279

Nuclear electric quadrupole moment:

non-spherical distribution of nuclear charge

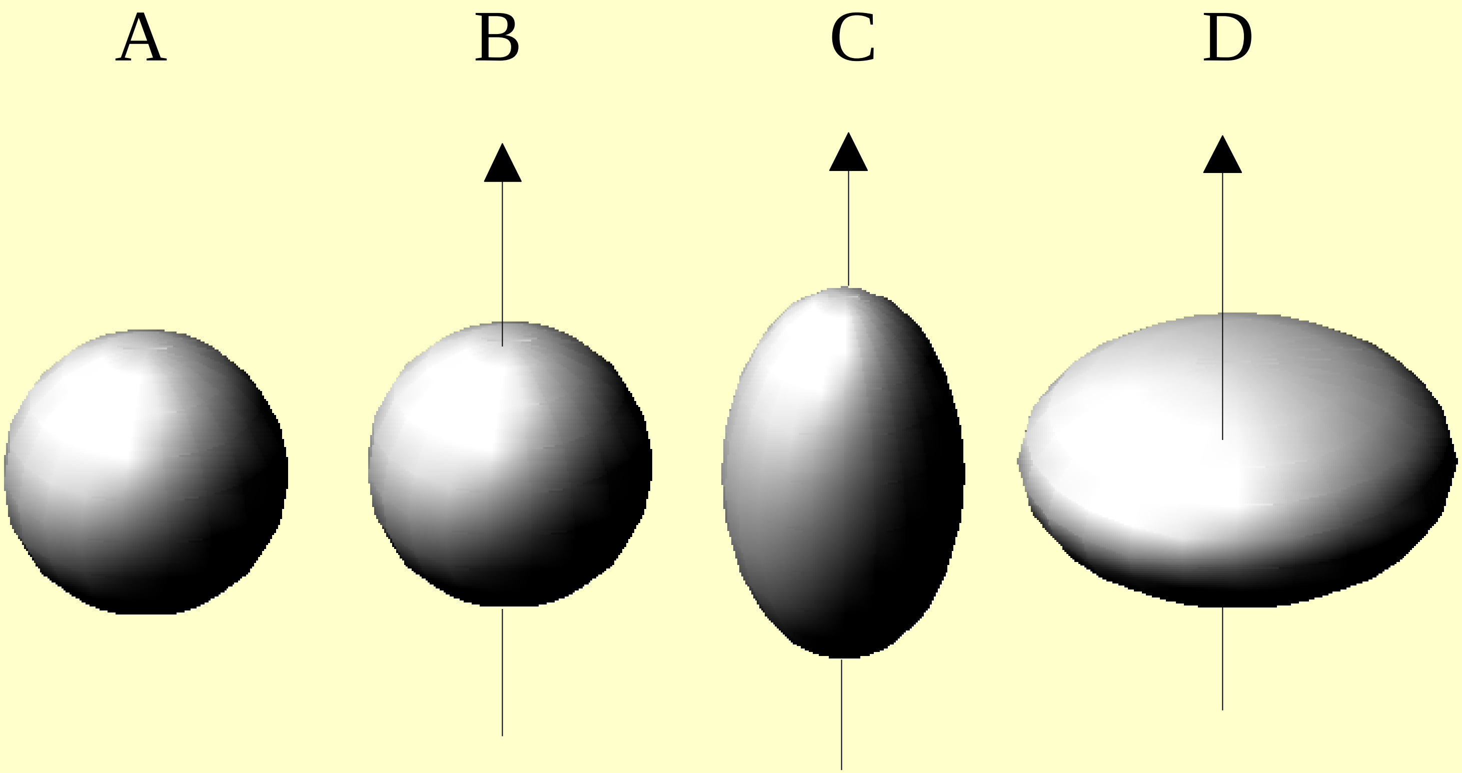

I = 0   I = 1/2   I ≧ 1 ; eQ > 0   I ≧ 1 ; eQ < 0

$eQ \sim 10^{-25}$ to 10^{-30} m^2

Outline

Solid State NMR – General Aspects

Anisotropic Interactions:

- magnetic shielding
- nuclear electric quadrupole coupling
- dipole-dipole coupling
- indirect spin-spin coupling

➡ **Manipulation of Interactions**

- magic-angle spinning
- cross-polarization
- -J-spectroscopy/INADEQUATE
- rotational echo double resonance

Solid State NMR

- element-selective
- locally selective
- quantitative
- experimentally flexible: Selective averaging

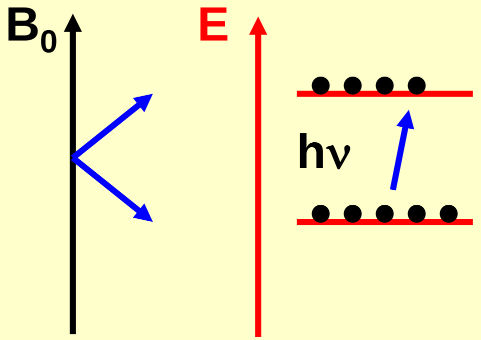

$$\Delta E = \gamma \hbar B_0$$

$$H = H_Z + H_D + H_{CS} + H_Q$$

Internucl. distances

Coordination numbers and symmetries

Magic Angle Spinning - MAS

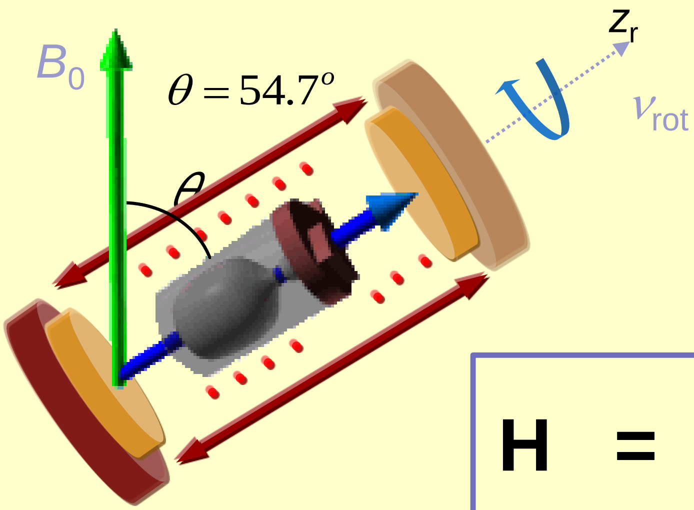

$$H_{aniso} = A \cdot \{3\,\overline{\cos^2\theta - 1}\}$$

$$H = H_Z + \cancel{H_D} + \cancel{H_{CS}}_{\,iso} + \cancel{H_Q}_{\,2nd.}$$

High-resolution spectra, governed by chemical shifts

-- bonding partners
-- coordination numbers

Magic Angle Spinning

$$\mathcal{H}_{aniso} = A \cdot \{\overline{3\cos^2\theta - 1}\}$$

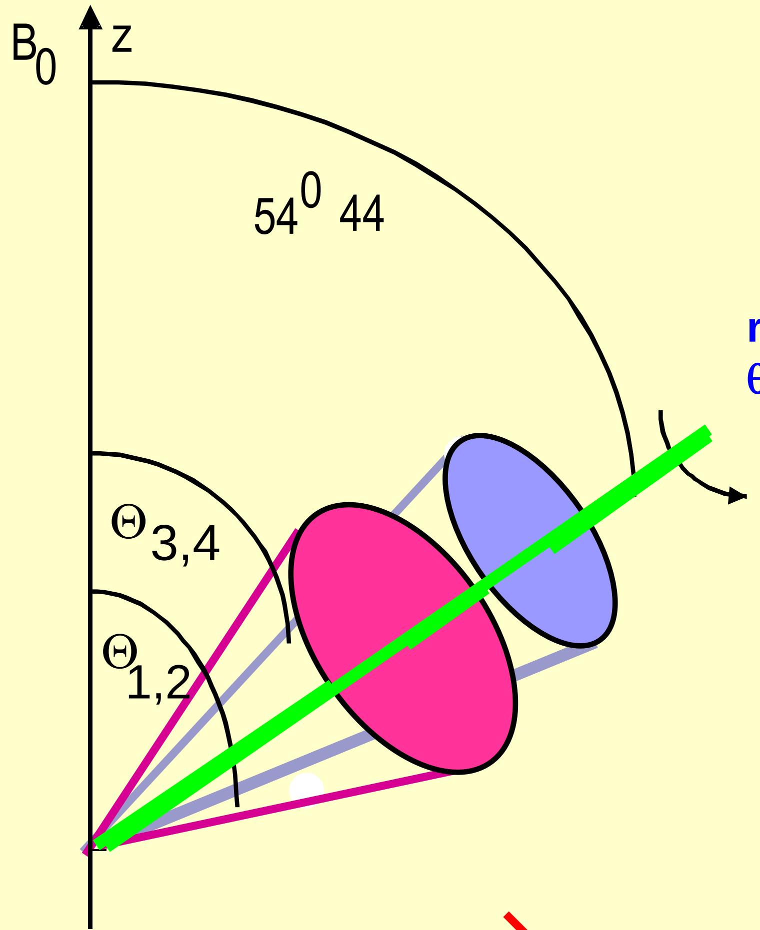

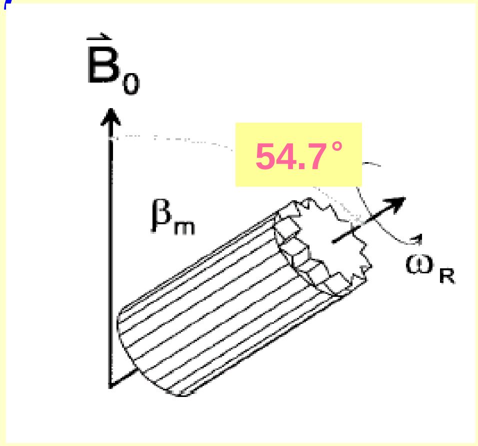

$$\mathcal{H} = \mathcal{H}_Z + \cancel{\mathcal{H}_D} + \cancel{\mathcal{H}_{CS}} + \cancel{\mathcal{H}_Q}$$

iso

2ª order

MAS-NMR probe

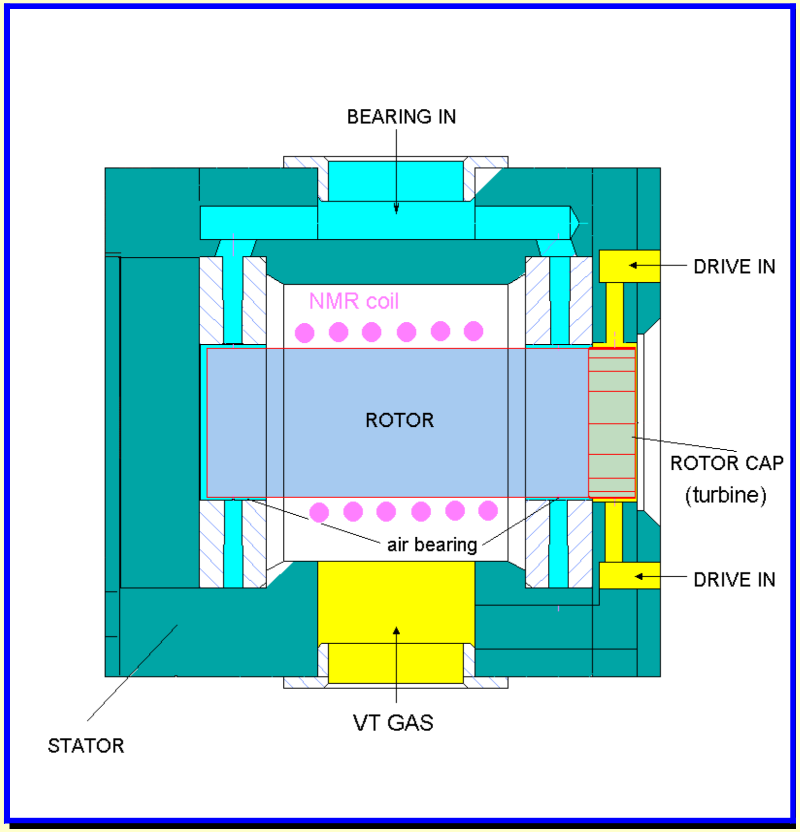

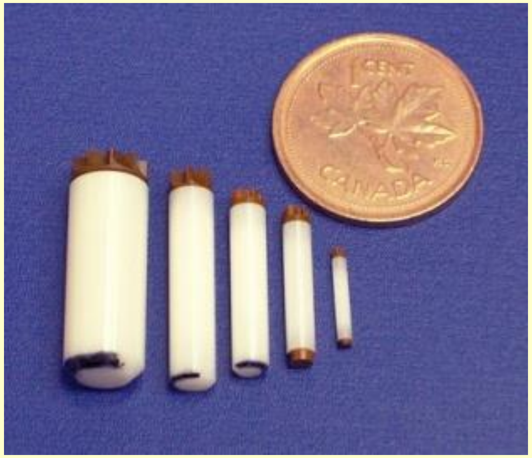

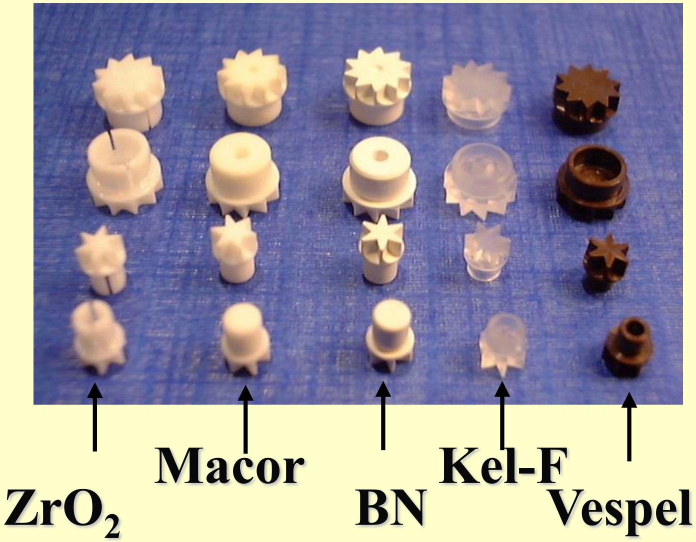

The effect of spinning speed

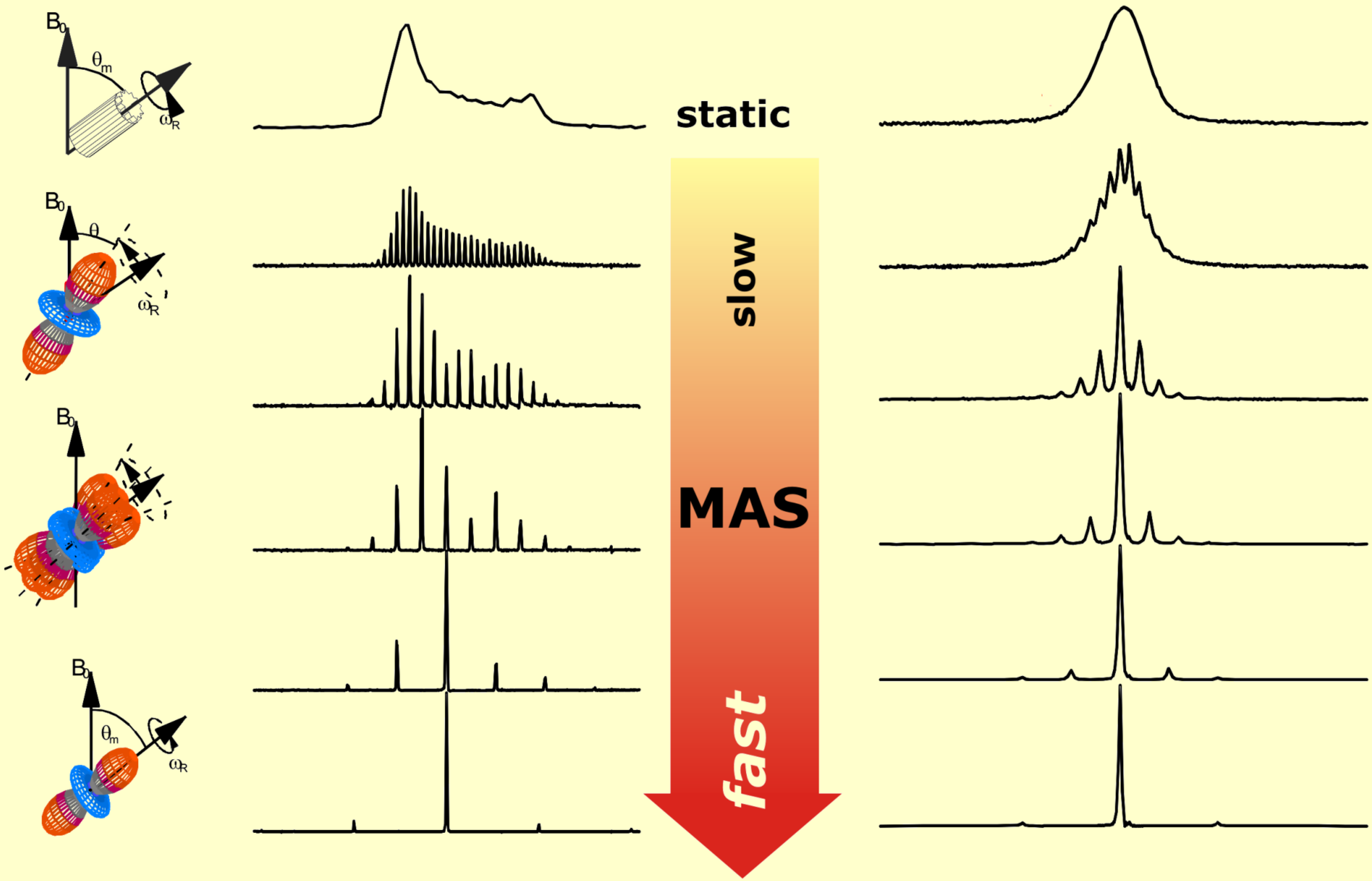

Nuclear electric quadrupole moment:

non-spherical distribution of nuclear charge

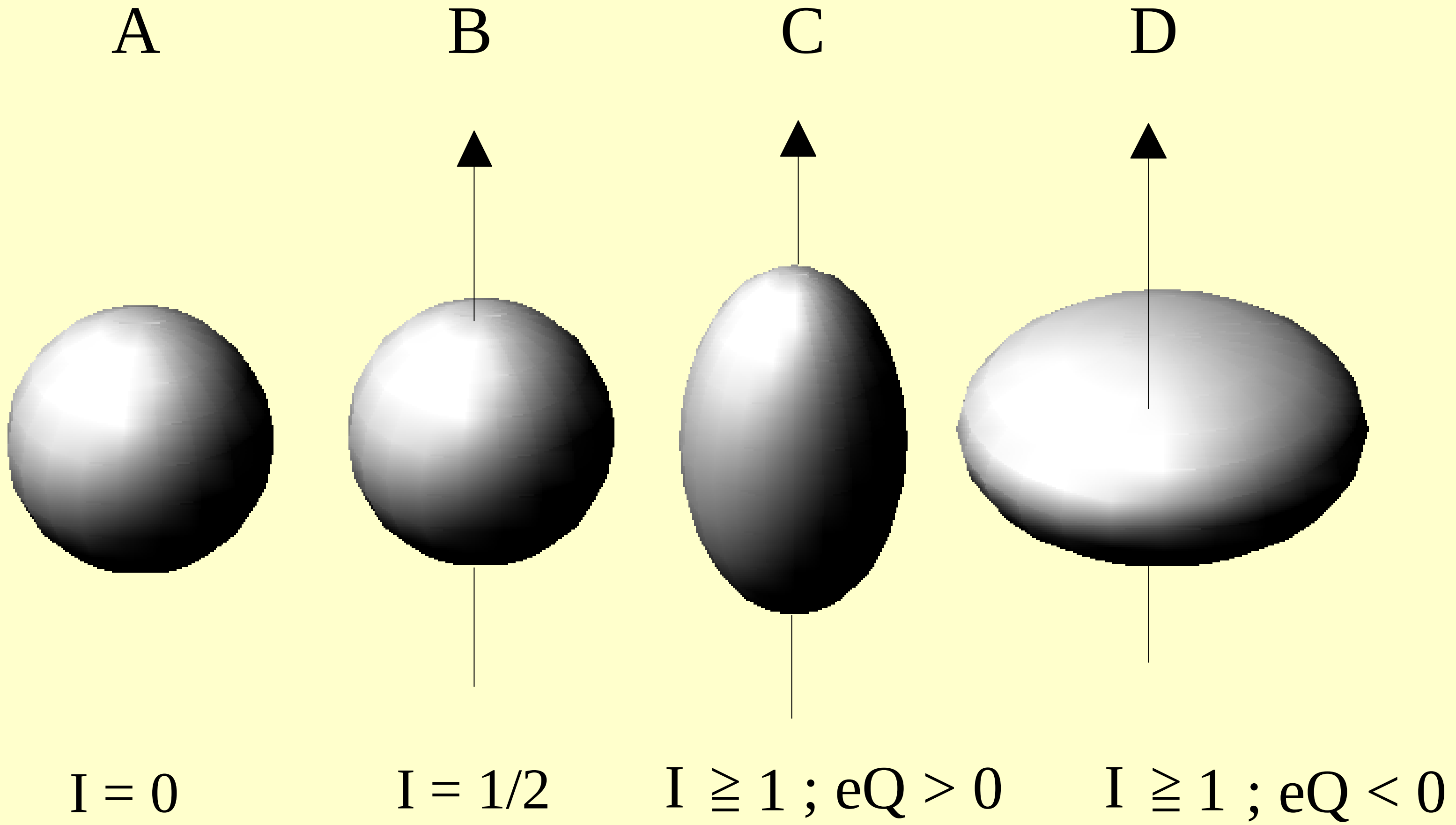

$eQ \sim 10^{-25}$ to 10^{-30} m^2

The physical picture

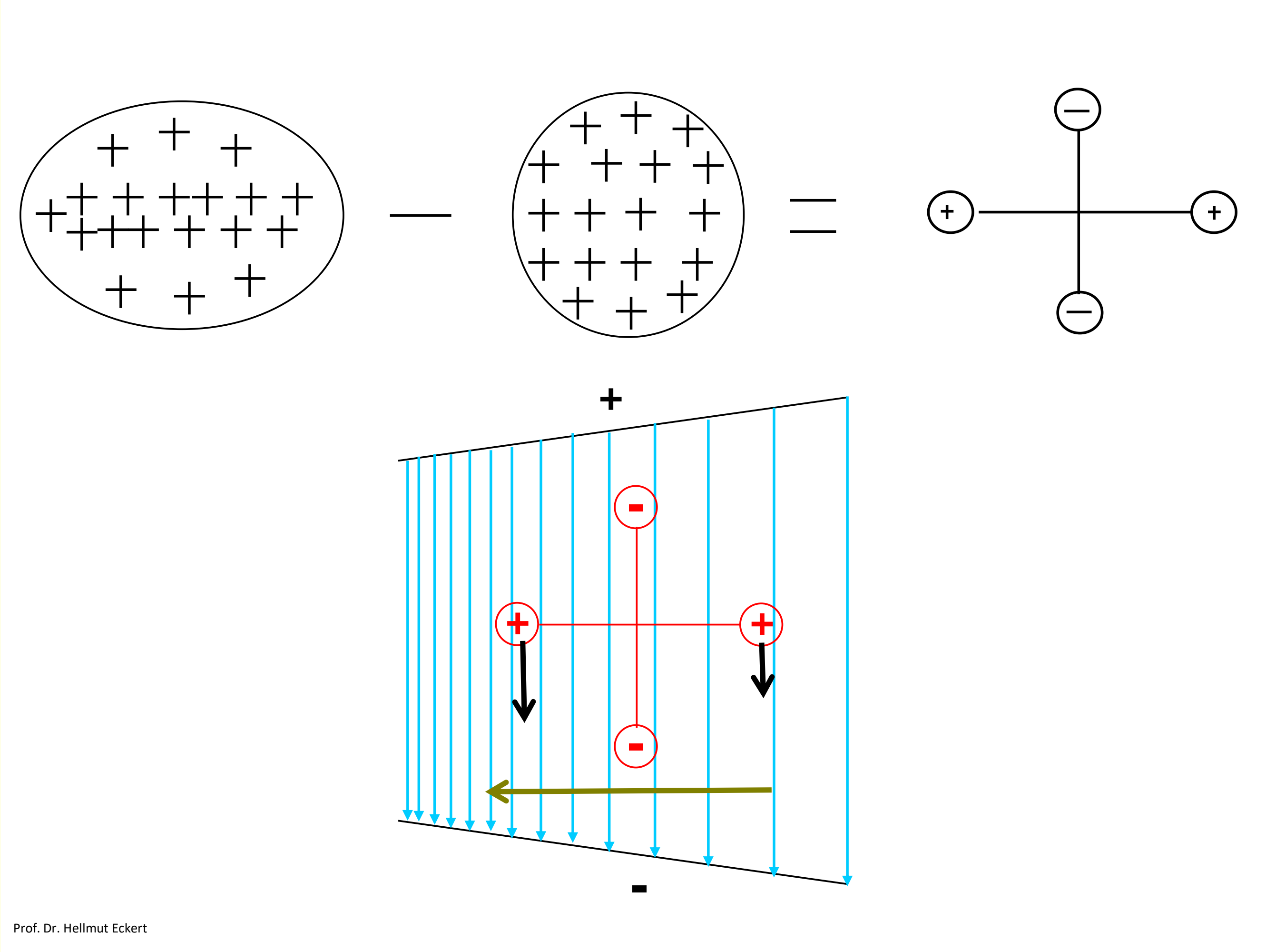

This quadrupole moment interacts with local electric field gradients created by the bonding environment of the nuclei.

-> probe of local symmetry

For axially symmetric EFG, the 1st order correction is:

$$\langle m|\hat{H}_Q|m\rangle = \frac{e^2qQ}{4I(2I-1)}\left[3m^2\cos^2\theta + \tfrac{3}{2}I(I+1)\sin^2\theta - \tfrac{3}{2}m^2\sin^2\theta - I(I+1)\right]$$

$$E_m^{(1)} = -m\gamma\hbar B_o + \frac{e^2qQ}{4I(2I-1)}\left[3m^2 - I(I+1)\right]\frac{3\cos^2\theta - 1}{2}$$

Energy level diagram for I = 3/2

Θ = 90°

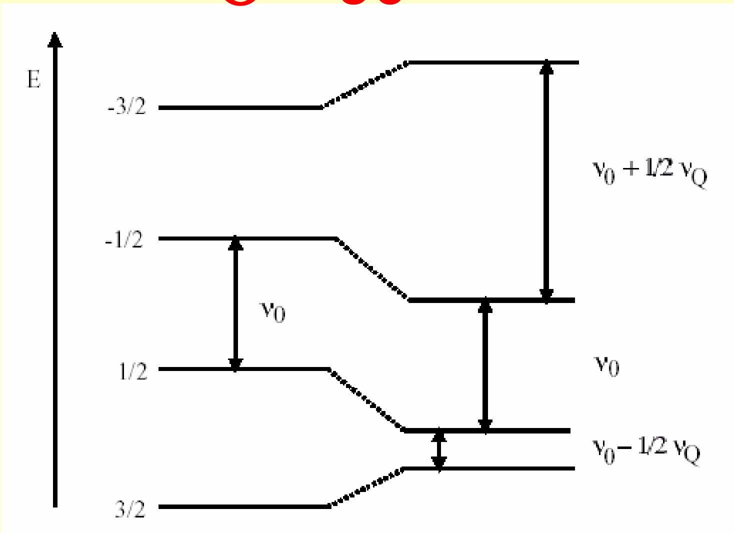

Θ = 0°

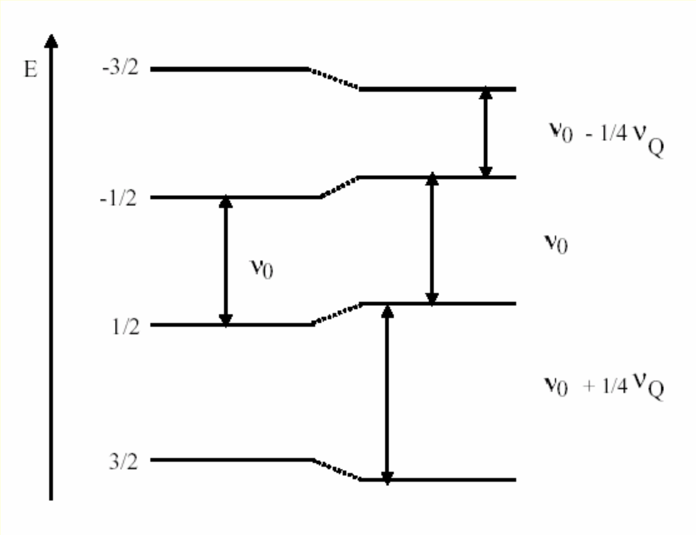

Powder samples: orientational averaging case I = 3/2

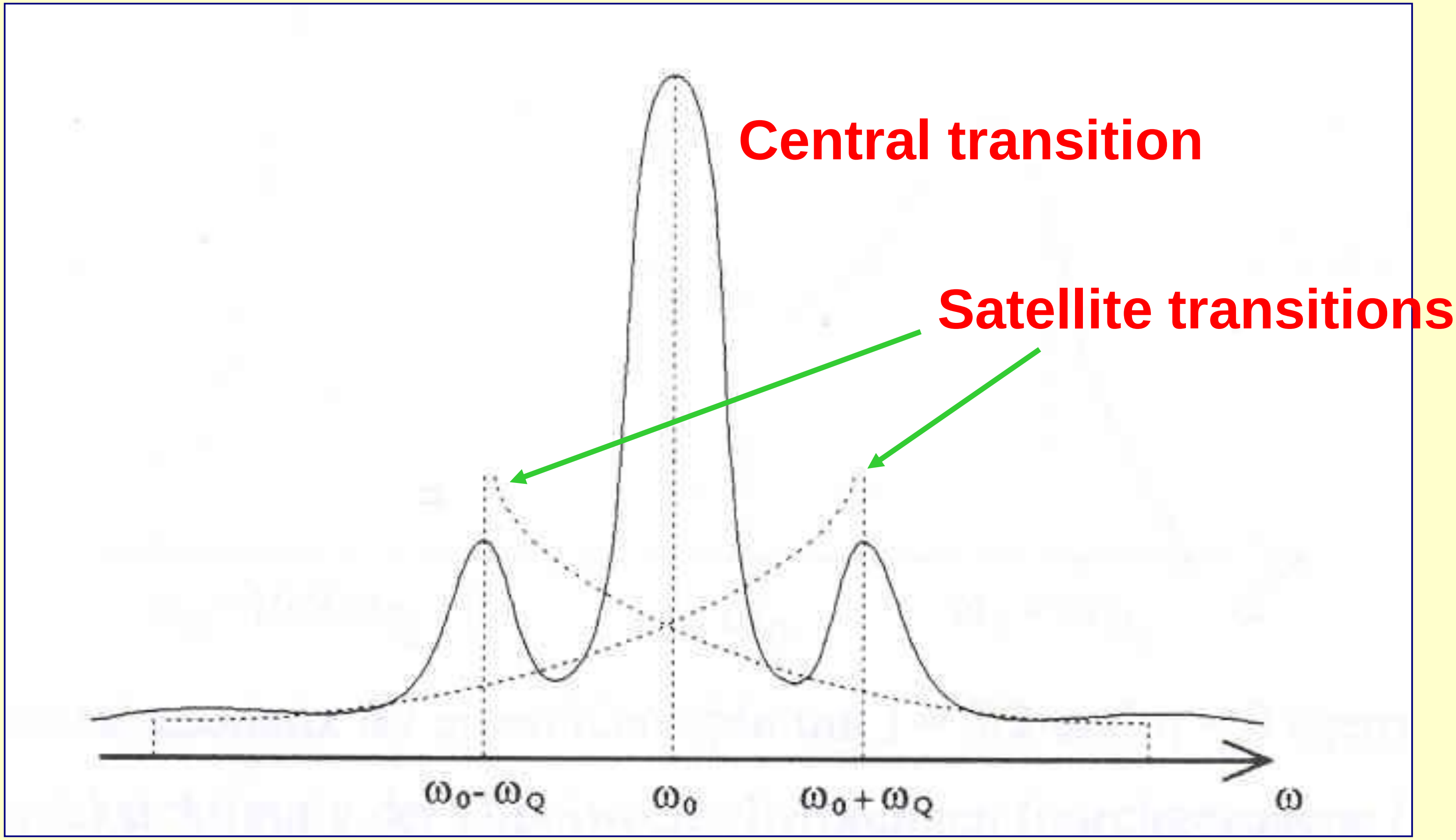

Powder pattern for spin-7/2

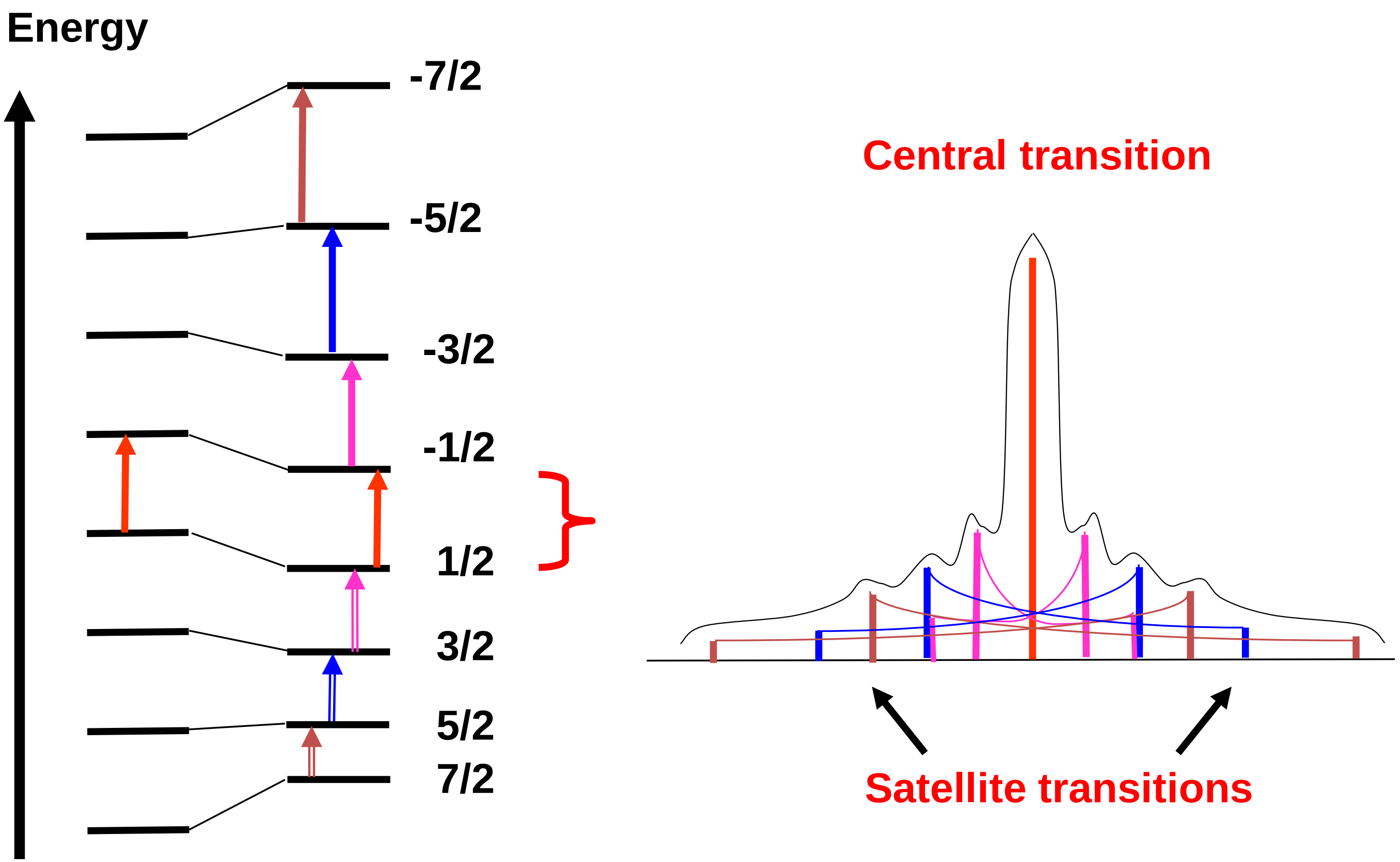

Stronger Quadrupole Coupling:

Second-order perturbation theory

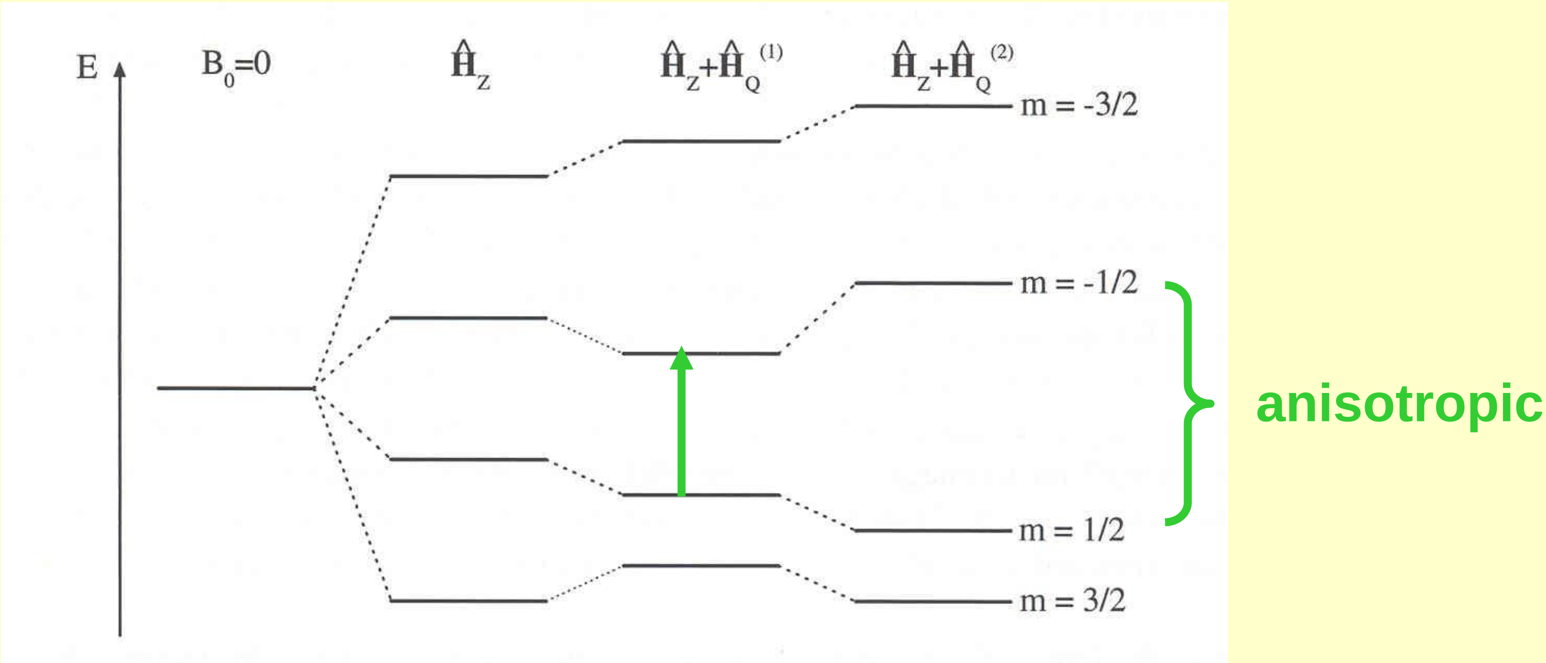

Solid State NMR Periodic Table

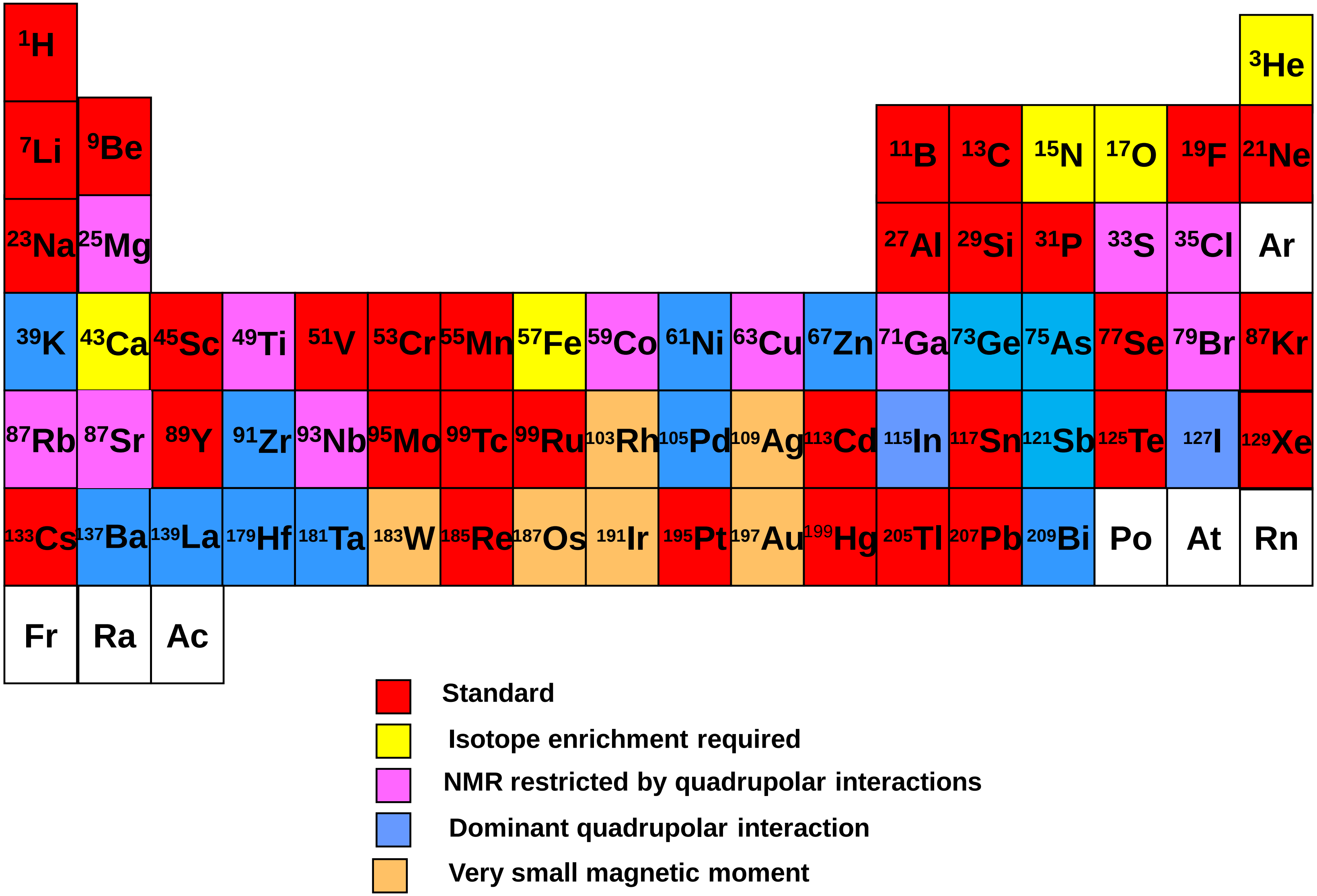

NMR as a Technique in Solid State Sciences

Local Selectivity:	Disorder/Lack of Periodicity
Element Selectivity:	Compositional Complexity Low Scattering Contrast (H; Si/Al)
Interaction Selectivity:	Distance Measurements Connectivity Information Electron Density Information
Uniform Sensitivity:	Quantitative Applications
Dynamic Sensitivity:	Motional Processes on Continuous Timescale (10^2 to 10^{-9} s)
Low Detection Sensitivity:	10^{17} to 10^{18} spins required
Bulk Method:	poor spatial resolution surfaces/interfaces difficult to study
Magnetic Interference:	transition metals, rare earths: limited

NMR spectroscopy of insensitive nuclei:

Problems with direct detection of ^{13}C, ^{15}N and others:

- **Low natural abundance**
- **Small magnetic moments**
- **Long spin-lattice relaxation times**

Basic idea of cross-polarization (CP):

exploit dipole-dipole coupling with abundant ^{1}H nuclei in the sample to transfer magnetization from ^{1}H to ^{13}C spins

Matching of energy levels required

(flip-flop mechanism), not possible in the lab frame

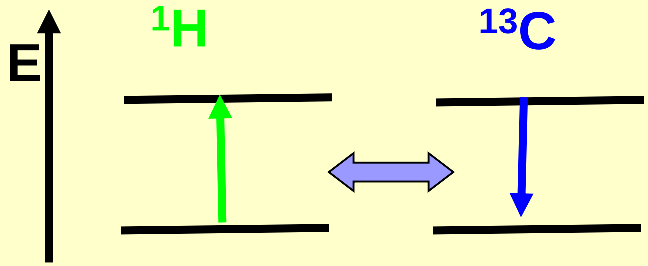

The crosspolarization pulse sequence

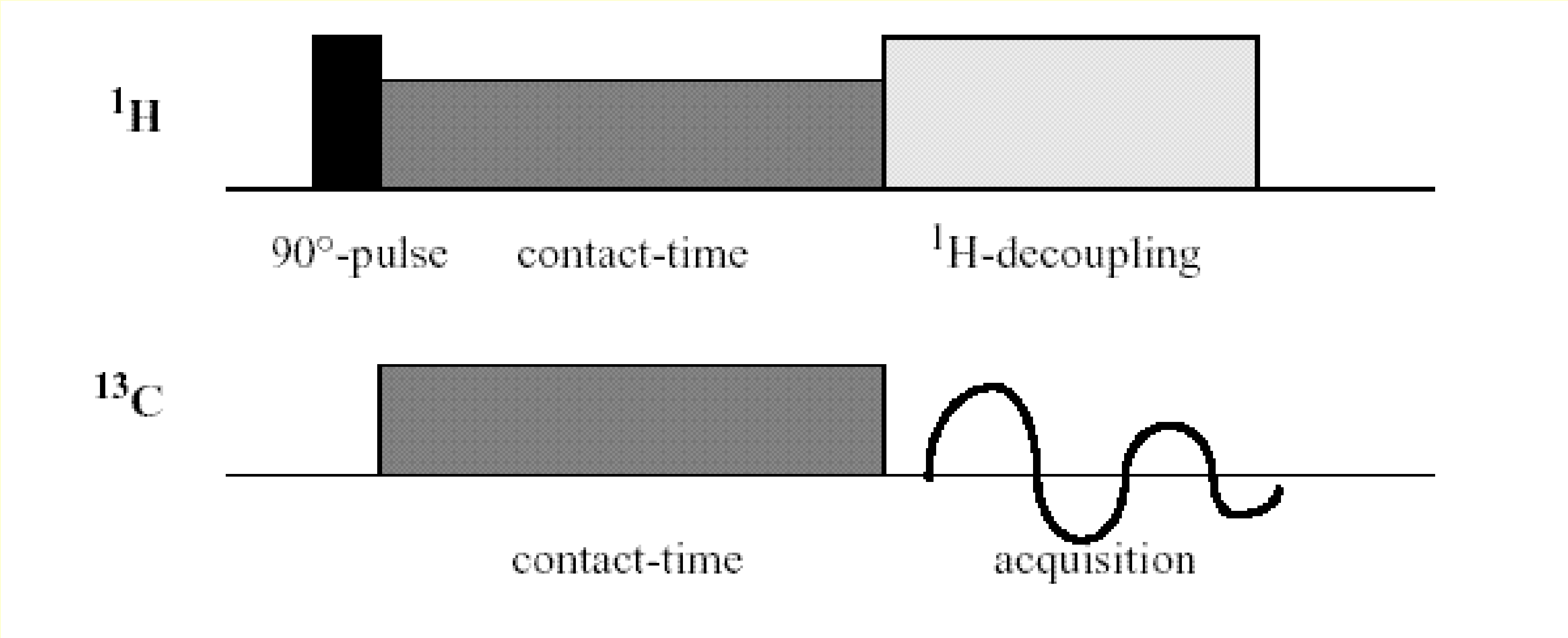

Hartmann-Hahn matching condition

$$\gamma_{1H} B_{1H} = \gamma_{13C} B_{13C}$$

^{13}C- NMR spectra of adamantane

static, no ^{1}H-decoupling

Δ=1000 Hz

static, with ^{1}H-decoupling

Δ=500 Hz

MAS, no ^{1}H-decoupling

Δ=50 Hz

MAS, with ^{1}H-decoupling

Δ= 5 Hz

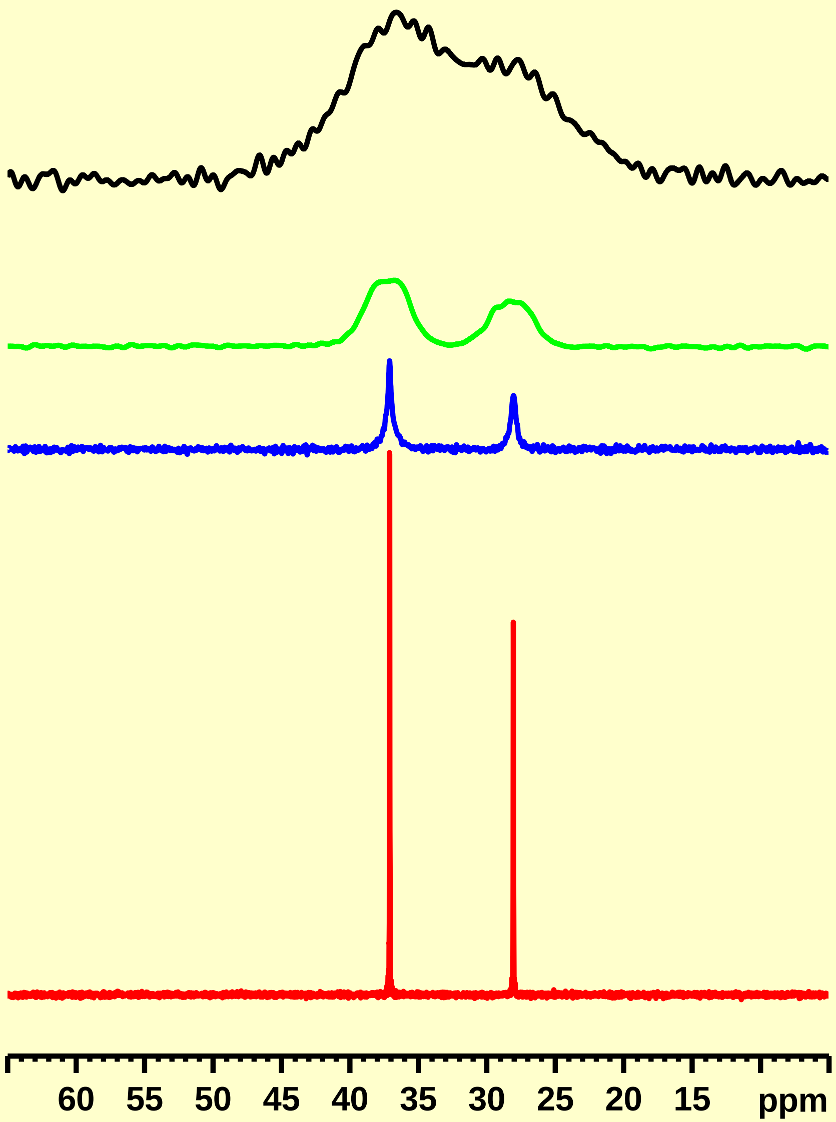

Poly-dicarbazolyl-hexadiyne (poly DCH)

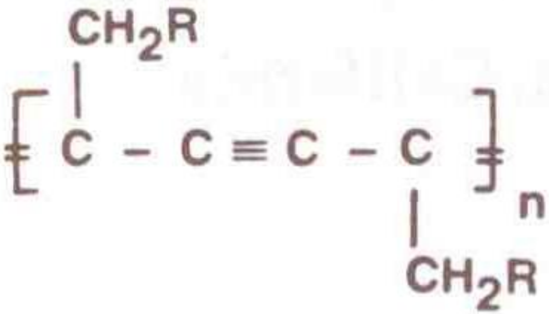

$$R - CH_2 - C \equiv C - C \equiv C - CH_2 - R$$

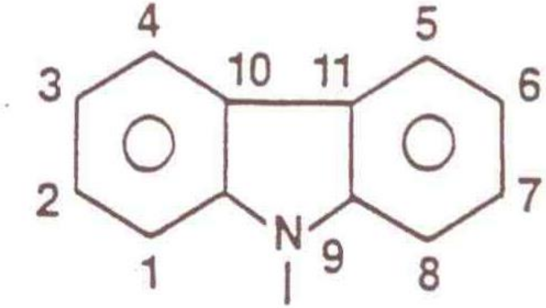

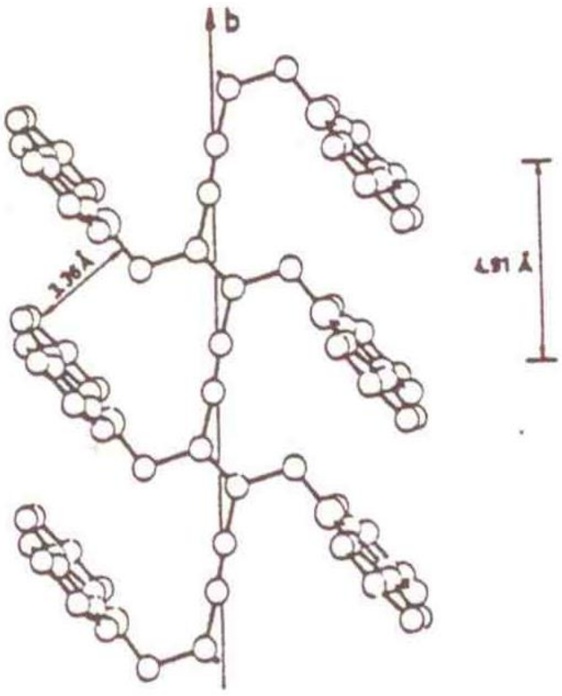

Variable Contact time experiments

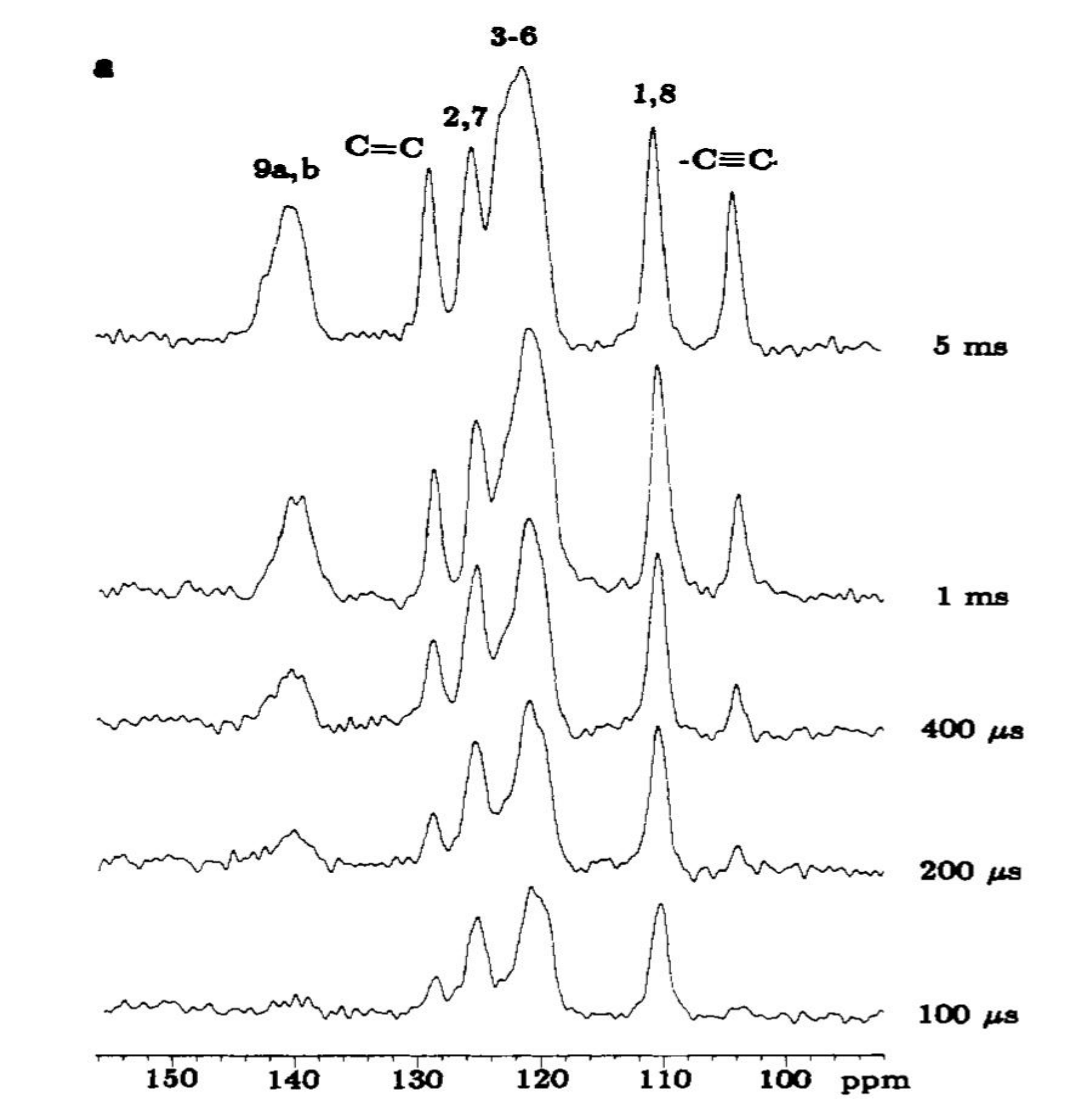

CP MAS with delayed decoupling

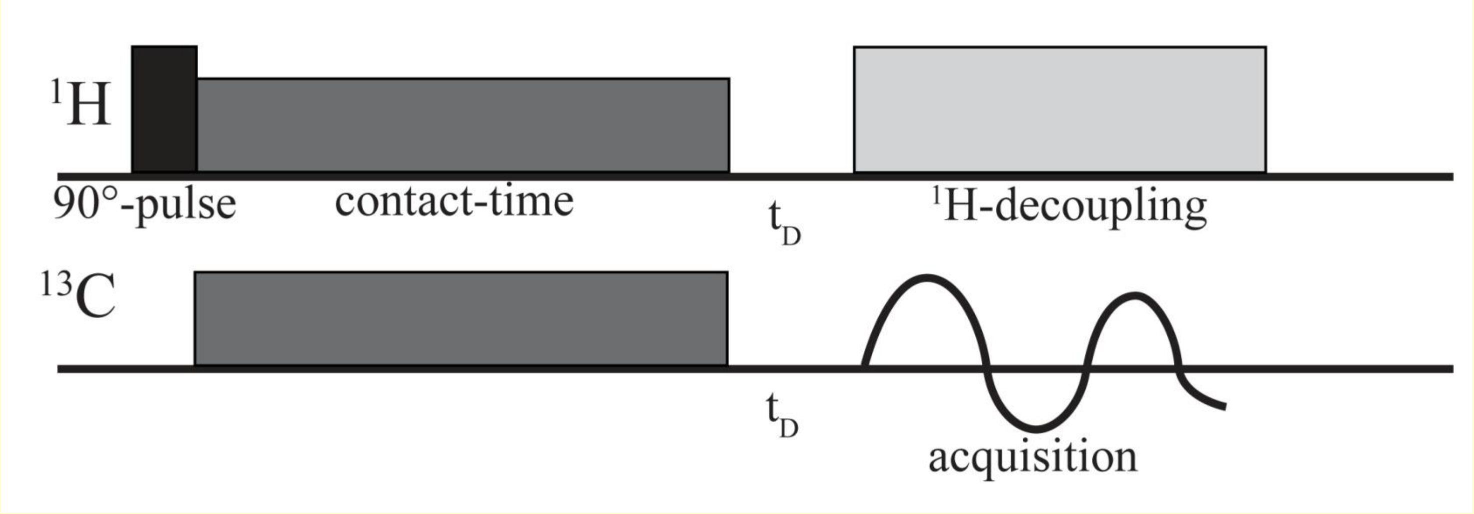

Selection of non-protonated and mobile C-atoms

CPMAS of poly-DCH

regular

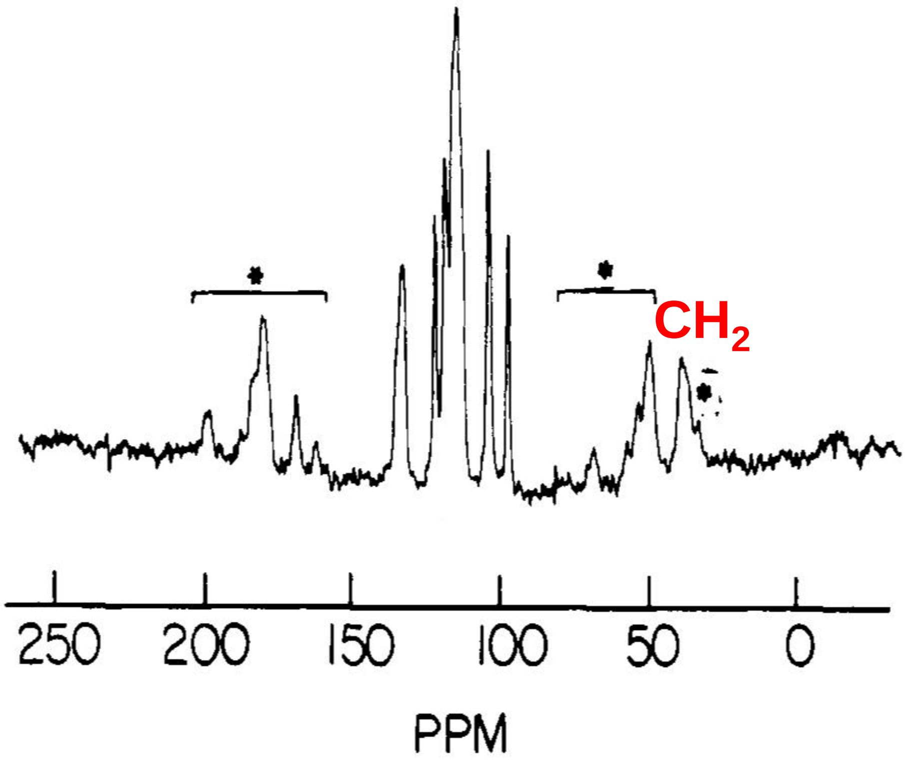

with delayed decoupling

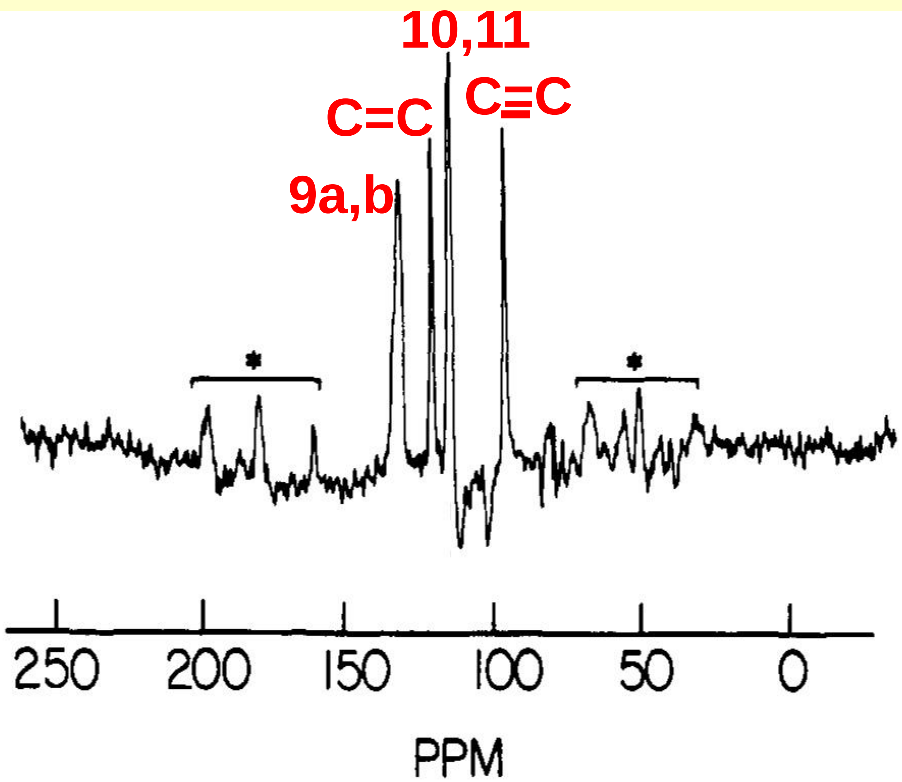

2-D Heteronuclear correlation NMR

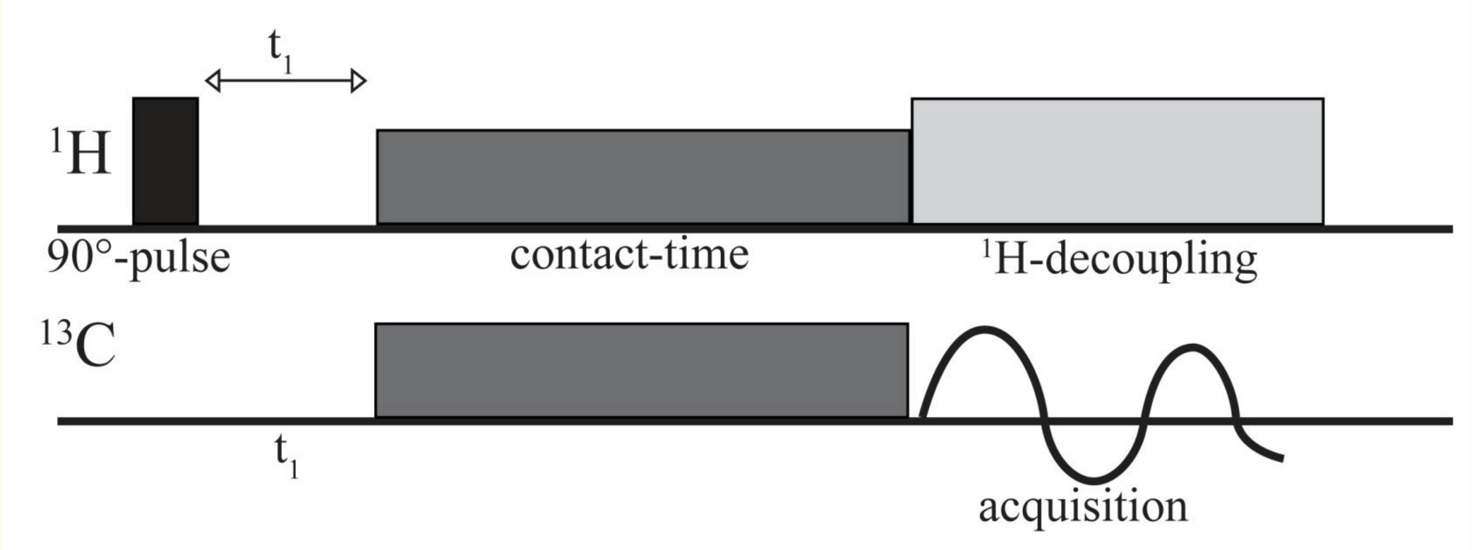

correlates the ^{13}C resonances with those ^{1}H species from which the magnetization is transferred the fastest = typically the directly bonded protons

High Resolution $^{1}H/^{13}C$ HETCOR

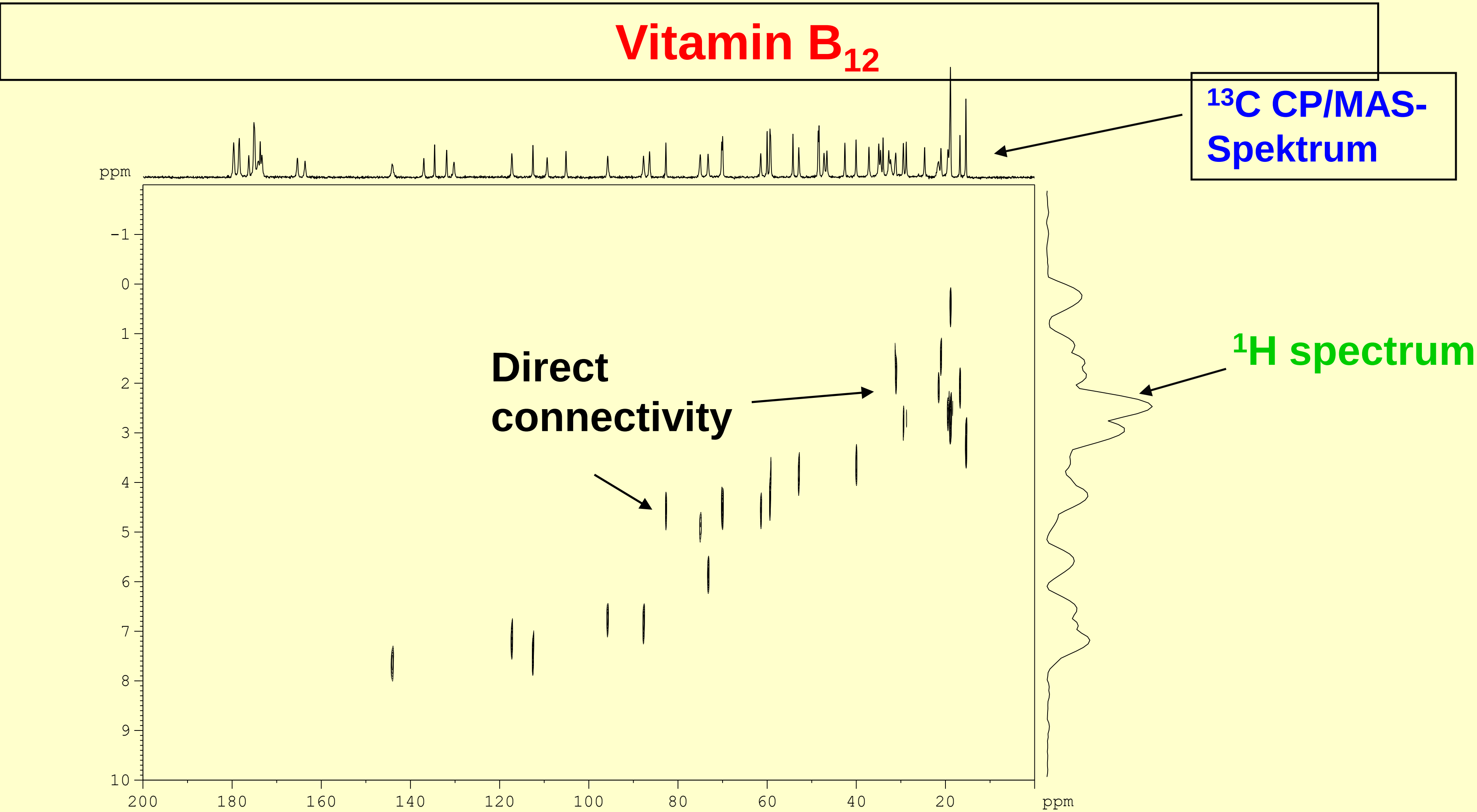

A Modern 2D HETCOR Sequence

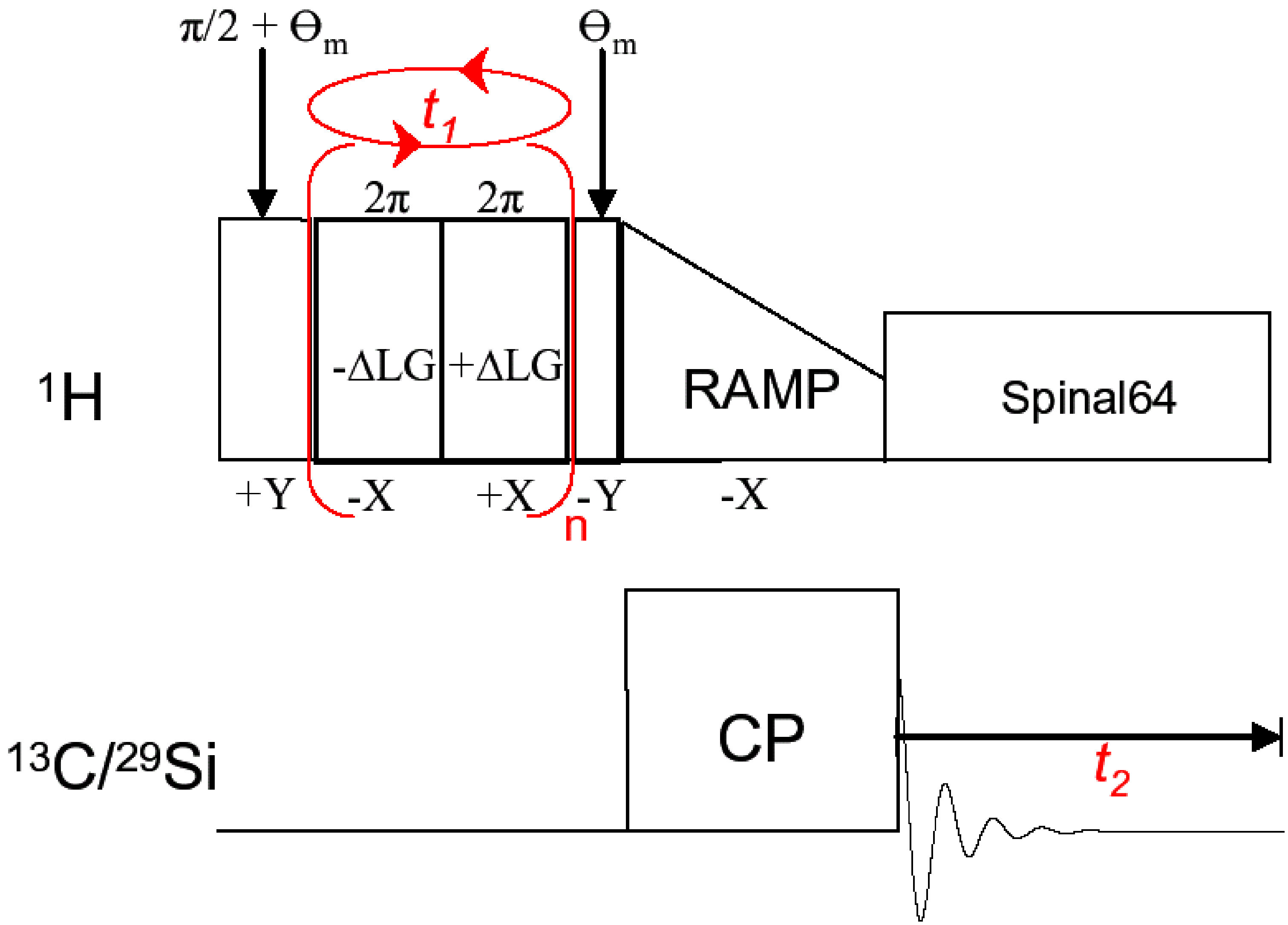

Hydrophobic Interaction
Propanolol/ormosil

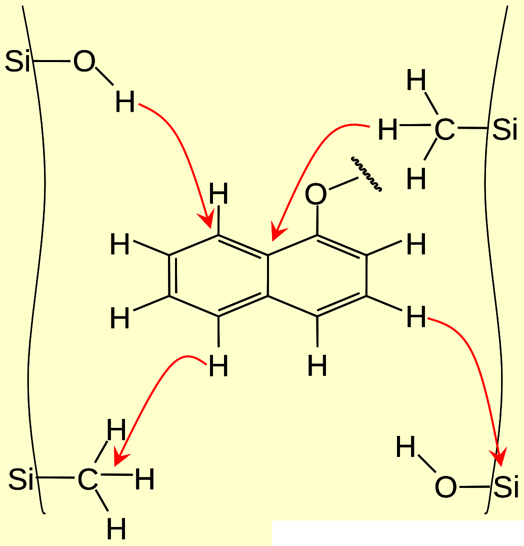

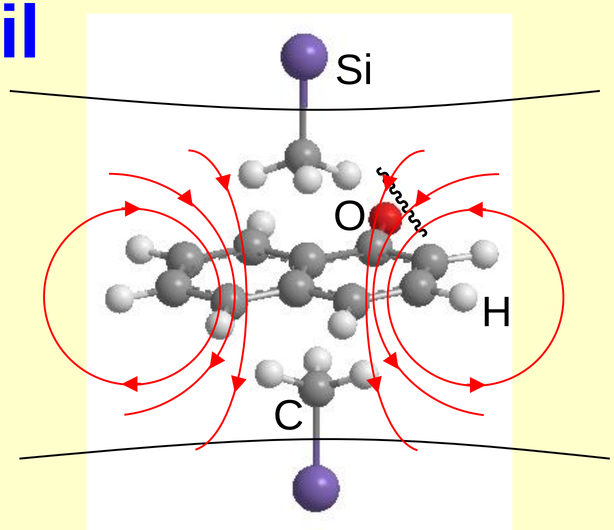

HETCOR data

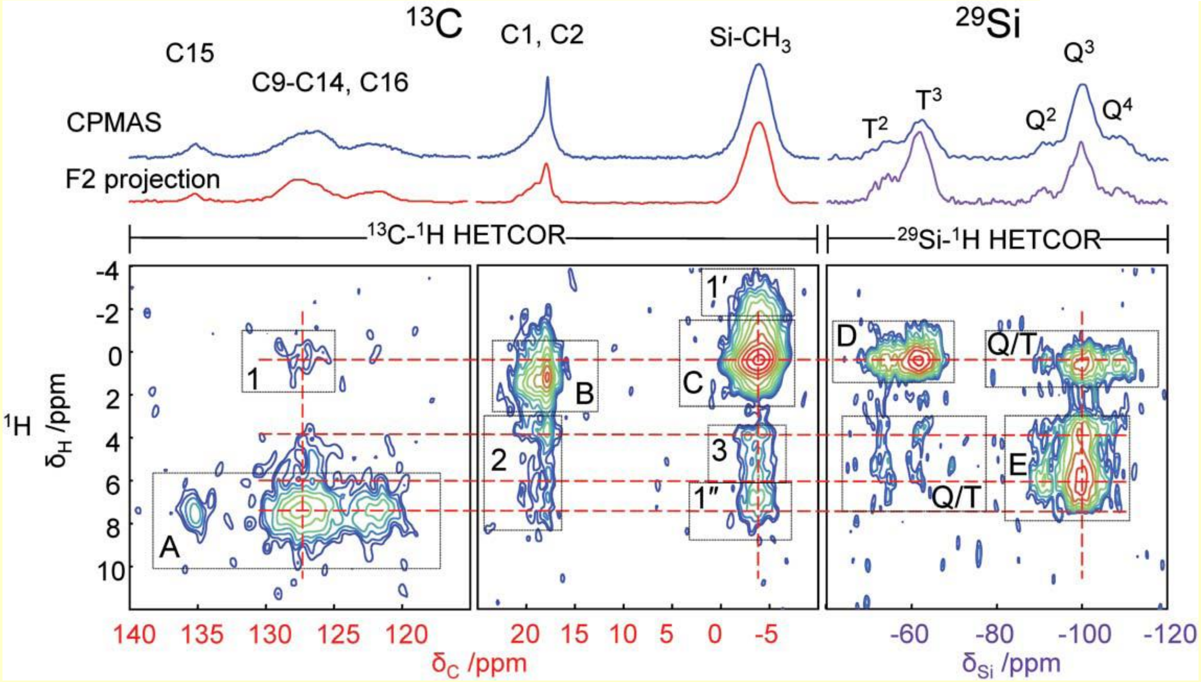

G. Paul, S. Steuernagel, H. Koller, *Chem. Commun.* **2007**, 5194

Cross-polarization dynamics

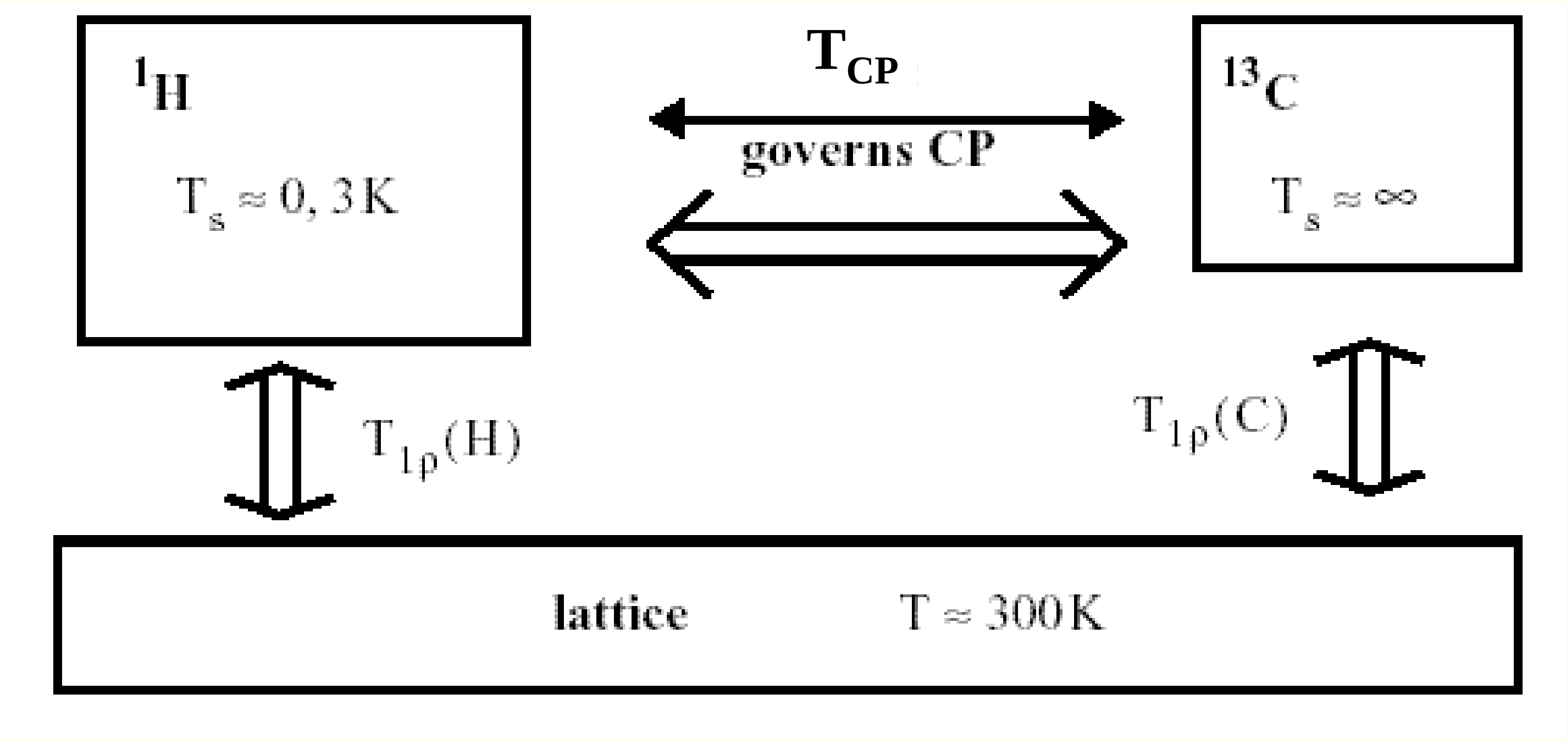

Variable contact time curves are influenced by three distinct time constants

Separate measurement of $T_{1\rho}(H)$

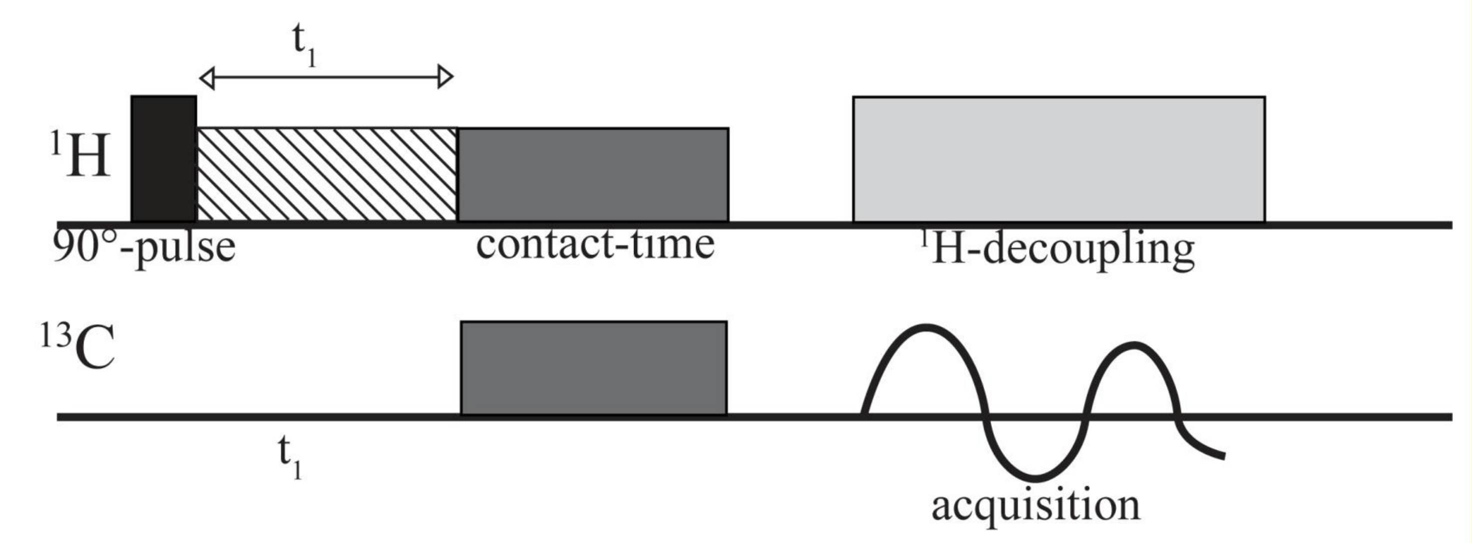

With the further assumption that $T_{1\rho}(^{13}C)$ is very long, these variable contact times can be fitted, yielding T_{CP}

$$I(t) = B(1 - T_{CP} / T_{1\rho}^{H})^{-1}\left[\exp(-t / T_{1\rho}^{H}) - \exp(-t / T_{CP})\right]$$

Variable Contact time Experiments in $^{29}Si\{^1H\}$ CPMAS of amorphous silica

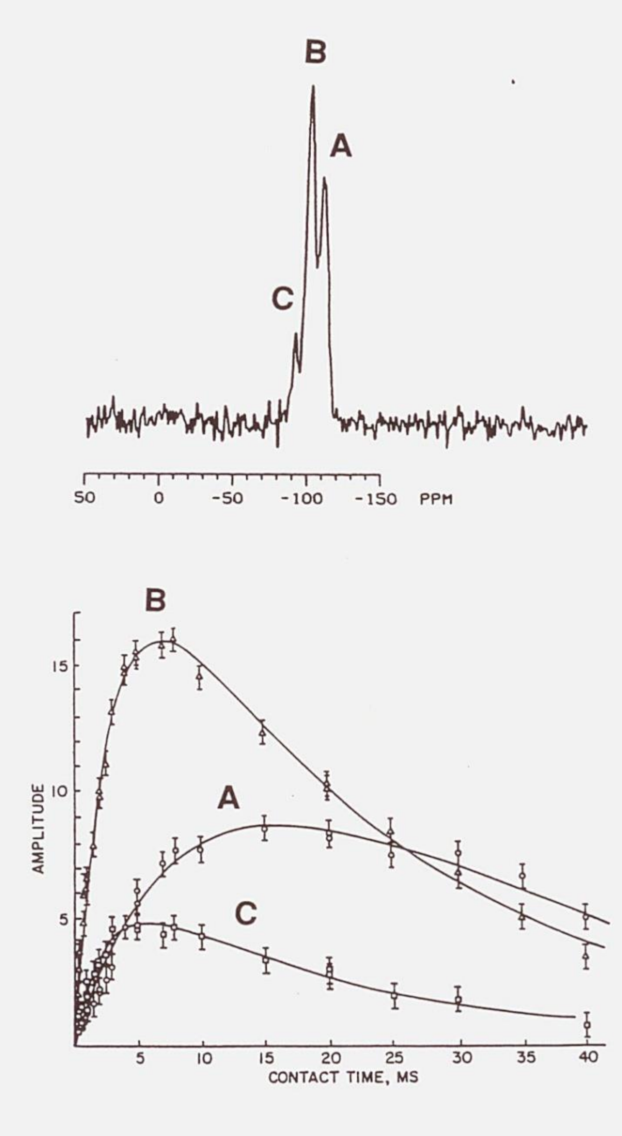

A = $SiO_{4/2}$
B = $SiO_{3/2}OH$
C = $SiO_{2/2}(OH)_2$

Electron-> Nuclear Dynamic Polarization (DNP)

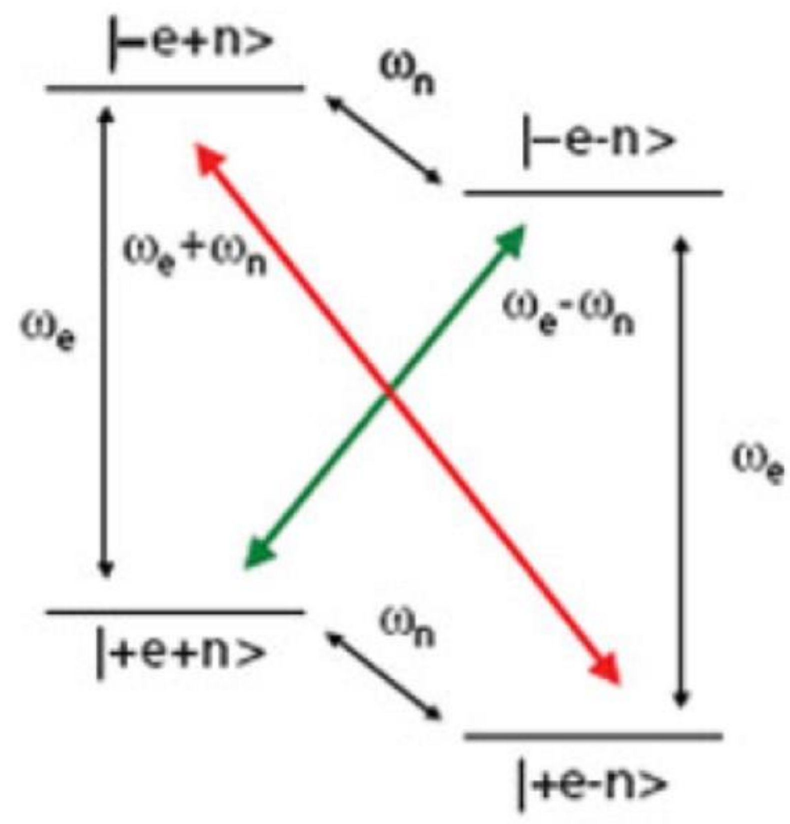

Organic Biradicals as nuclear polarizers

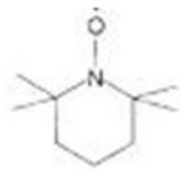

TEMPO

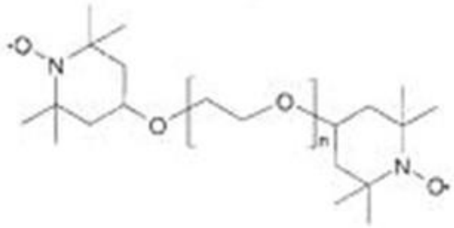

BTnE
n=2,3,4

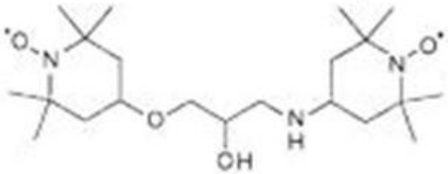

TOTAPOL

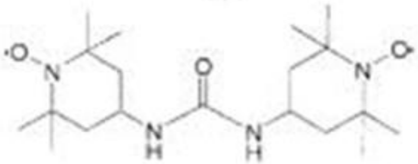

BTurea

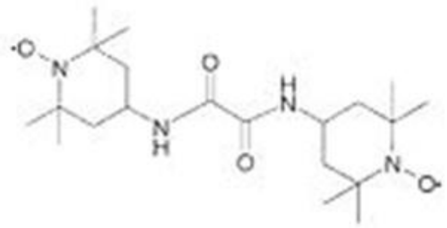

BTOXA

Pulse Sequence for Dynamic Nuclear Polarization

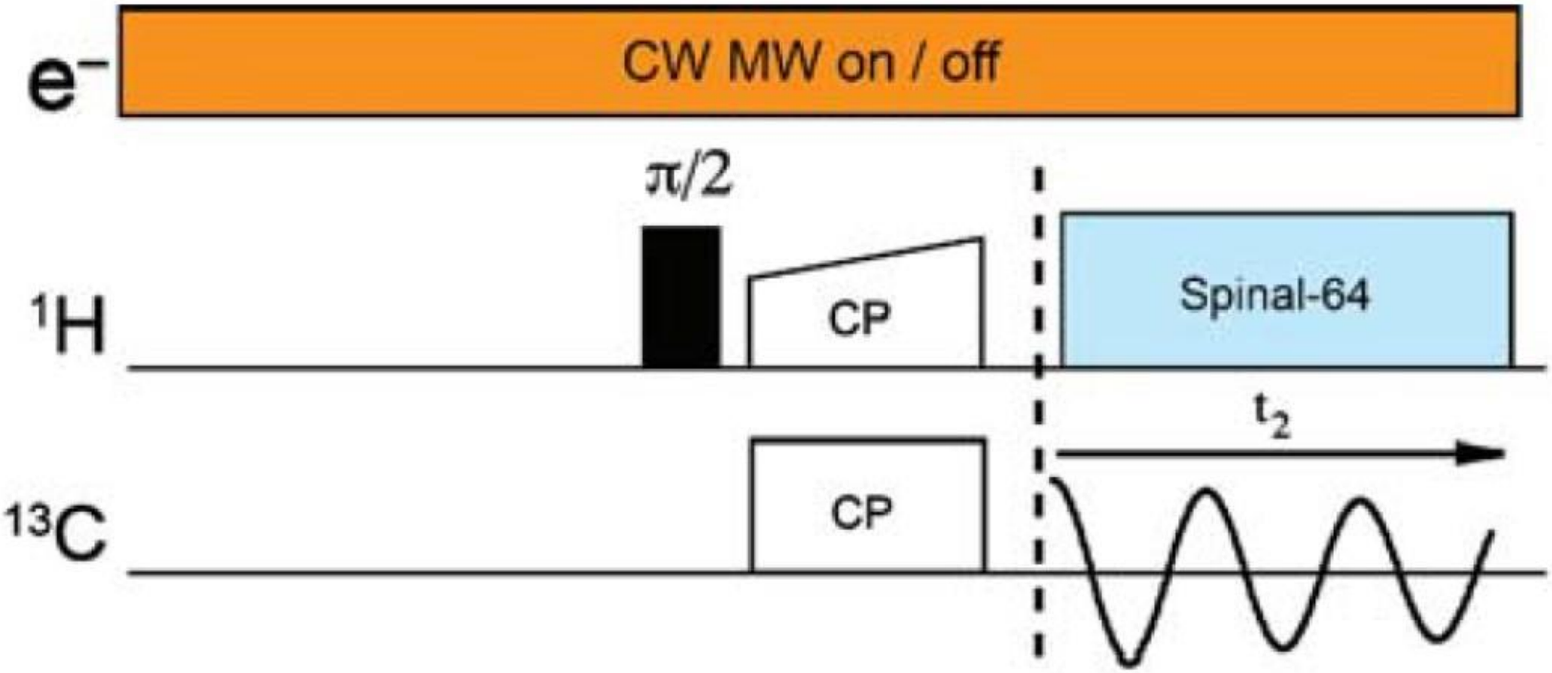

An application: surface selective NMR:
Functionalization of MCM silica surface

DNP enhanced ^{13}C-NMR